

DISSANAYAKE, BUPATHI S., M.S. Effects of Altered Folate Metabolism on Specific Gene Expression in the Developing *Xenopus* Embryo. (2006)  
Directed by Dr. Karen S. Katula. 73pp.

Approximately 1 out of every 2000 births in the United States is affected by neural tube defects. The most well-known environmental cause of neural tube malformation is folate deficiency in pregnant women. The underlying mechanism for this relationship is unclear. The goal of this study was to determine if altered folate metabolism during early development leads to changes in the expression of selected genes. *Xenopus laevis* embryos were treated with different concentrations of homocysteine (0.5 mM, 1 mM, 10 mM, 25 mM, 50 mM and 100 mM) and methotrexate (1  $\mu$ M, 10  $\mu$ M, 50  $\mu$ M, 100  $\mu$ M and 200  $\mu$ M) and their gross morphology, direction of gut coiling and neural tube thickness were analyzed. At higher concentrations both compounds caused morphological defects, including delayed development, kinked bodies, reduced body size and lack of gut structure. The percent of guts coiling to the left decreased from 93% to 5% as the homocysteine concentration increased from 0 mM to 10 mM. Meanwhile the guts coiling to the right increased from about 5% to 39%. The percent of guts deformed or mis-coiled increased from 5% to 100%, with the homocysteine concentration increasing from 0 mM to 50 mM. Methotrexate also affected the morphology and direction of gut coiling in a concentration dependent manner. The thickness of the dorsal side of the neural tube of the methotrexate treated embryos decreased from about 6 mm to 3 mm as the concentration increased from 0  $\mu$ M – 200  $\mu$ M. The effect of homocysteine on the neural tube thickness was less clear. Gross

morphological effects and gut coiling suggest treatment of embryos with homocysteine and methotrexate affect embryos in a similar manner consistent with folate deficiency. *In situ* hybridization was performed on treated and untreated embryos to analyze changes in expression patterns of *Dkk-1*, *Pax-3*, *Xbra*, *Xtwist* and *Wnt-5A* genes. Gene expression patterns of *Xbra* and *Xtwist* were not affected by folate deficiency whereas *Dkk-1* and *Pax-3* expression appear to be down regulated. *Wnt-5A* data were inconclusive. These findings suggest that specific gene expression changes may be associated with folate deficiency. More studies are required to confirm these results.

EFFECTS OF ALTERED FOLATE METABOLISM ON SPECIFIC  
GENE EXPRESSION IN THE DEVELOPING  
*XENOPUS* EMBRYO

by

Bupathi S. Dissanayake

A Thesis Submitted to  
the Faculty of the Graduate School at  
The University of North Carolina at Greensboro  
In Partial Fulfillment  
of the Requirements for the Degree  
Master of Science

Greensboro  
2006

Approved by

---

Committee Chair

## APPROVAL PAGE

This thesis has been approved by the following committee of the Faculty of The Graduate School at The University of North Carolina at Greensboro.

Committee Chair \_\_\_\_\_

Committee Members \_\_\_\_\_

\_\_\_\_\_

\_\_\_\_\_  
Date of Acceptance by Committee

\_\_\_\_\_  
Date of Final Oral Examination

## TABLE OF CONTENTS

	Page
LIST OF TABLES .....	iv
LIST OF FIGURES .....	v
LIST OF ABBREVIATIONS.....	vi
CHAPTER	
I. INTRODUCTION .....	1
II. MATERIALS AND METHODS .....	16
III. RESULTS .....	26
IV. DISSCUSION .....	58
REFERENCES.....	70

## LIST OF TABLES

	Page
<b>Table 1.</b> Characteristics of Genes used for <i>In situ</i> Hybridization Studies.....	21
<b>Table 2.</b> Survival, General Appearance and Gut Coiling of Homocysteine Treated Embryos.....	32
<b>Table 3.</b> Survival and General Appearance of Methotrexate Treated Embryos .....	37
<b>Table 4.</b> Gut Coiling and the Appearance of Methotrexate Treated Embryos .....	38

## LIST OF FIGURES

	Page
<b>Figure 1.</b> Folate Pathway.....	4
<b>Figure 2.</b> Development of <i>Xenopus</i> Embryos Treated with Homocysteine.....	28
<b>Figure 3.</b> Development of <i>Xenopus</i> Embryos Treated with Methotrexate.....	30
<b>Figure 4.</b> Direction of Gut Coiling in Embryos Treated with Different Concentrations of Homocysteine .....	34
<b>Figure 5.</b> Examples of Gut Coiling.....	35
<b>Figure 6.</b> Direction of Gut Coiling in Embryos Treated with Different Concentrations of Methotrexate.....	40
<b>Figure 7.</b> Analysis of the Neural Tube.....	42
<b>Figure 8.</b> Neural Tube Thickness at Different Homocysteine Concentrations.....	43
<b>Figure 9.</b> Neural Tube Thickness at Different Methotrexate Concentrations.....	44
<b>Figure 10.</b> Expression Pattern of <i>Pax-3</i> in Treated and Untreated Embryos.	47
<b>Figure 11.</b> Expression Pattern of <i>Pax-3</i> in Treated and Untreated Embryos Under High Magnification. ....	48
<b>Figure 12.</b> Expression Pattern of <i>Dkk-1</i> in Treated and Untreated Embryos.....	50
<b>Figure 13.</b> Expression Pattern of <i>Dkk-1</i> in Treated and Untreated Embryos Under High Magnification.....	51
<b>Figure 14.</b> Expression Pattern of <i>Xtwist</i> in Treated and Untreated Embryos.....	53
<b>Figure 15.</b> Expression Pattern of <i>Xtwist</i> in Treated and Untreated Embryos Under High Magnification .....	54
<b>Figure 16.</b> Expression Pattern of <i>Xbra</i> in Treated and Untreated Embryos.....	55
<b>Figure 17.</b> Expression Pattern of <i>Xbra</i> in Treated and Untreated Embryos Under High Magnification.....	56

## LIST OF ABBREVIATIONS

<b>5,10 MTHFR</b>	5,10-methylenetetra-hydrofolate reductase
<b>5-methyl-THF</b>	5-methyltetrahydrofolate
<b>AICAR</b>	aminoimidazole-4-carboxamide ribonucleotide
<b>BCIP</b>	5-bromo-4-chloro-3-indolylphosphate
<b>BMBR</b>	Boehringer Blocking Reagent
<b>DEPC</b>	diethylpyrocarbonate
<b>Dkk-1</b>	Dickkopf-1
<b>dTMP</b>	deoxythymidine monophosphate
<b>dUMP</b>	deoxyuridylate monophosphate
<b>EtOH</b>	ethanol
<b><i>Folbp1</i></b>	folate binding protein 1
<b>formyl-THF</b>	formyltetrahydrofolate
<b>GAR</b>	glycinamide ribonucleotide
<b>HEPES</b>	N-2-hydroxyethylpiperanziner-N'-2-ethanesulfonic acid
<b>hpf</b>	hours past fertilization
<b>LS</b>	lamb serum
<b>MAB</b>	maleic acid buffer
<b>MBS</b>	modified Barth's Saline
<b>MEMF</b>	MOPS/EGTA/magnesium sulfate/formaldehyde
<b>MeOH</b>	methanol
<b>MetSyn</b>	methionine synthase
<b>MOPS</b>	N-morpholino propanesulfonic acid
<b>NaAcetate</b>	sodium acetate
<b>NBT</b>	nitro blue tetrazolium
<b>NTD</b>	neural tube defects
<b><i>Pax-3</i></b>	Paired box gene-3
<b>PBS</b>	phosphate-buffered saline
<b>PBST</b>	1X PBS and 0.1% Tween-20
<b>RT-PCR</b>	reverse transcription polymerase chain reaction
<b>SAM</b>	S-adenosyl methionine
<b>SSC</b>	sodium citrate
<b>TEA</b>	triethanolamine
<b>TMP</b>	thymidylate monophosphate
<b>TS</b>	thymidylate synthase
<b>Xbra</b>	<i>Xenopus</i> brachyury
<b>Xtwist</b>	<i>Xenopus laevis</i> twist



# CHAPTER I

## INTRODUCTION

Folate is a water soluble B vitamin that has to be obtained from the diet.

Numerous disorders have been associated with folate deficiency. These include neural tube defects (NTDs) (Smithells *et al.*, 1976; Lucock *et al.*, 1998), occlusive vascular disease (OVD) (Refsum *et al.*, 1998; Petri *et al.*, 1996), cleft palate (Bienengraber *et al.*, 2001), Alzheimer's disease (Clarke *et al.*, 1998), Down's syndrome (James *et al.*, 1999), unexplained premature births (Dekker *et al.*, 1995), colon, breast, cervical and bronchial cancers (Butterworth, 1993; Kamei *et al.*, 1993; Slattery *et al.*, 1999), and heart defects (Tang *et al.*, 2004; Li *et al.*, 2005). The molecular basis for the relationship between folate deficiency and these different conditions remains unclear.

Approximately 1 out of every 2000 births are affected by neural tube defects, the most common, severely disabling birth defects in the United States. The most well-known environmental cause of neural tube malformation is folate deficiency in pregnant women (Northrup and Volcik, 2000). It is estimated that consumption of 0.4 mg of folic acid per day by pregnant women can reduce the number of neural tube defects by 48% (Daly *et al.*, 1995). It has yet to be determined how folate deficiency increases the risk of NTD's and other developmental defects.

The goal of this study was to determine if altered folate metabolism during early development leads to changes in the expression of selected genes. Embryos were treated

with different concentrations of homocysteine and methotrexate, compounds known to affect the folate pathway. Gross morphological changes, direction of the gut coiling, and alterations in neural tube fusion were analyzed in these embryos. Using conditions determined by this initial study, embryos treated with methotrexate and homocysteine were analyzed for changes in gene expression by *in situ* hybridization. Genes used in this study included two known to be involved in neuroectoderm differentiation and morphogenesis, *Xtwist* and *Pax-3*, the latter of which is known to be affected by folate deficiency (Tang *et al.*, 2003), two genes known to be affected by folate deficiency in a cell culture system (*Dkk-1* and *Wnt-5A* (Katula, submitted)), and a control gene not associated with neuroectoderm (*Xbra*).

This study is significant because an observed change in the expression of these genes would suggest that folate deficiency or conditions that mimic folate deficiency can affect the expression of specific genes. This could be the underlying cause of developmental defects associated with folate deficiency.

## **Background**

### ***Folate Metabolism and Function***

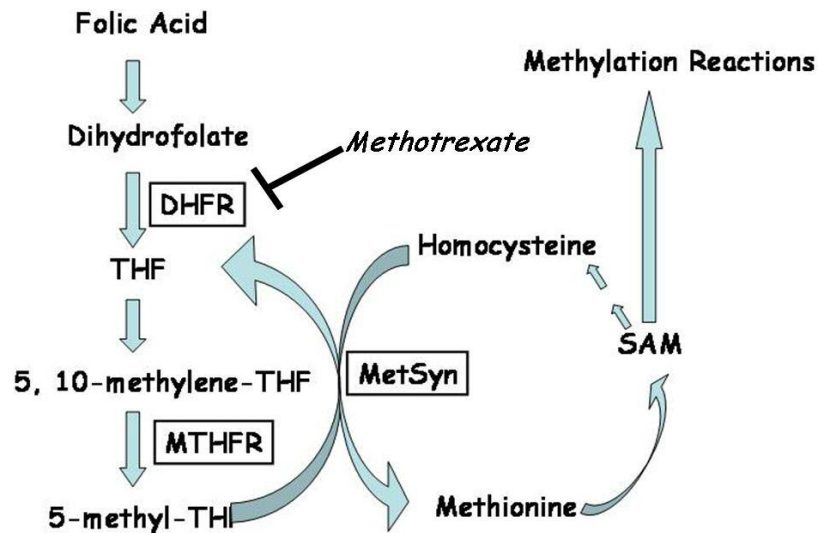
Folic acid or pteroylmonoglutamate is the parent structure of folates, a family of chemically similar, highly unstable compounds. Folates facilitate the transfer of one-carbon units from donor molecules on to various substrates of important biosynthetic pathways, such as synthesis of thymidylate, methionine and purine, conversion of serine to glycine, and the catabolism of histidine (Lucock, 2000). Humans can not synthesize

folate and it must be obtained from folate rich foods including yeast extracts such as marmite, liver, kidney, citrus fruits and leafy green vegetables.

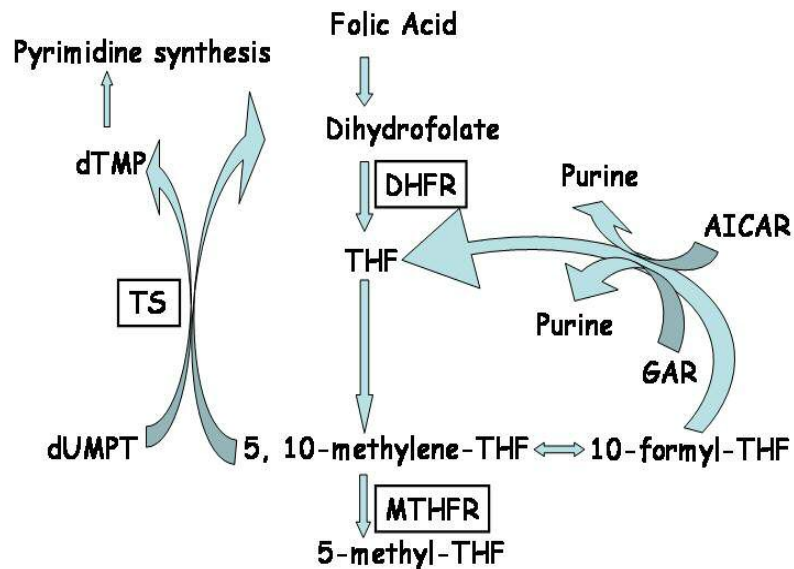
Dietary folates, mostly existing as 5-methyltetrahydrofolate (5-methyl-THF) and formyltetrahydrofolate (formyl-THF), are transported across the enterocyte brush border membrane through an anion exchange anti-port transporter (Lucock *et al.*, 1989; Herbert *et al.*, 1962). Polyglutamyl folates are metabolized in the liver into monoglutamyl folate, 5-methyl-THF, which is then transported in the serum to the peripheral tissues. Transport of folate into the cells depends on two systems; membrane carriers and specific folate binding proteins. In most cells the folate binding proteins are the primary mode of transport. After binding of the folate to the carriers, the complex is internalized by a nonclathrin-mediated endocytotic pathway (Birn *et al.*, 1993).

5-methyl-THF acquired by diet or by reduction of 5,10-methylene-THF by flavoprotein 5,10-methylenetetra-hydrofolate reductase (5,10 MTHFR) is required for the methylation of homocysteine to methionine by vitamin B12 dependent methionine synthase (MetSyn) (Fig. 1A). The resulting methionine can be converted into S-adenosyl methionine (SAM) by methionine adenosyltransferase. SAM functions as a methyl donor in a variety of reactions, including methylation of DNA and proteins (Fig. 1A).

During purine synthesis, aminoimidazole-4-carboxamide ribonucleotide (AICAR) transformylase and glycinamide ribonucleotide (GAR) transformylase transfer a one-carbon unit to AICAR and GAR, respectively, from 10-formyl-THF (Fig. 1B). These one-carbon units become carbon atoms 2 and 8 of the developing purine ring. In pyrimidine biosynthesis, the methylation of deoxyuridylylate monophosphate (dUMP) by



A) Methylation of Homocysteine to Methionine.



B) Purine and Pyrimidine Biosynthesis.

**Figure 1. Folate Pathway:** Folic acid is converted into different folate compounds as it moves through the folate pathway. Methotrexate inhibits dihydrofolate reductase (DHFR) which blocks the folate pathway from that point on (A). As a result, methylation of homocysteine to methionine is prevented, increasing the homocysteine concentration. A metabolite of folate pathway, 5, 10-methylene-THF, is required in purine and pyrimidine synthesis (B).

5,10-methylene-THF is catalyzed by thymidylate synthase (TS) to produce thymidylate monophosphate (TMP), which is used in pyrimidine synthesis (Fig. 1B).

Clearly, the biochemical consequences of folate deficiency have broad cellular consequences. The reduction in nucleotide precursors leads to decreased rates of DNA synthesis and reduced DNA repair capacity and associated increases in double strand DNA breaks (Blount *et al.*, 1997; Duthie *et al.*, 2000). On the other side of the pathway (Fig. 1B), an increase in homocysteine results from lack of the metabolite 5,10-methylene-THF and there is a decrease in the cellular level of SAM. This causes a reduction in DNA and protein methylation reactions. Global hypomethylation and changes in gene specific methylation have been detected in folate deficient cells (Pufulete *et al.*, 2003). Consequently, there is an increase in gene silencing and in some studies increased gene expression (Lucock, 2000). Increased oxidative stress in the form of free radicals has also been associated with excess homocysteine (Racek *et al.*, 2005; Romerio *et al.*, 2005). These findings suggest that more than one mechanism is contributing to the link between folate deficiency and different developmental defects.

### ***Xenopus laevis as a Model System***

For many years amphibians have been used in research to understand cellular, molecular and developmental mechanisms. For numerous reasons, *Xenopus laevis*, the African clawed frog, is an ideal model system for such research. These animals were first introduced to United States in 1940s. Initially, they were used in laboratories to check for pregnancy; injection of urine from a pregnant woman induces these frogs to lay eggs.

Since then *Xenopus laevis* has become one of the predominantly used species in embryology, as well as molecular and cellular biology (Wilt and Hake, 2004).

The *Xenopus* eggs are relatively large, about 1 mm in diameter, and the embryos develop outside the animal. This permits the easy manipulation and examination of these embryos. Because of their large size the embryo is suitable for a wide variety of molecular and cellular techniques including *in situ* hybridization, single cell injection of antibodies or RNA and cell ablation studies. Up to the first 12 cell divisions, mitosis occurs about every 30 min, producing an embryo with over 4000 cells in 3 hours (Wilt and Hake, 2004). As a result of their rapid development, researchers can obtain results rather quickly. In addition, the females produce eggs in large numbers and the adult animals are relatively easy to maintain.

All vertebrate embryos go through similar developmental stages during early embryogenesis. It has become clear that cellular and molecular mechanisms associated with development are conserved among vertebrate species and that proteins involved in these pathways perform similar biological functions (Gamse and Sive, 2000). Therefore, studies that can not be done in mammals can be carried out in lower vertebrates as a means to understand the biology of humans. Together, these characteristics and features make *Xenopus laevis* an ideal system to investigate the link between folate deficiency, gene expression and developmental defects.

## ***Neurulation***

Neurulation occurs during early embryogenesis of chordates and includes the formation of the neural plate, neural folds, and the neural tube. The formation of the neural plate starts with the induction of the neural plate or neural induction. By default, ectodermal cells become neuroepithelium. During neural induction, a suppressive signal produced by Hensen's node (equivalent to Spemann's organizer in amphibians) binds to secreted ligands such as bone morphogenetic proteins (BMP) or Wnts and blocks their function. This leads to suppression of the epidermal fate and formation of neuroectoderm. As the neural plate develops, the apicobasal thickening of the ectoderm results in a flat, thickened epithelial. This apicobasal thickening occurs as a result of cell elongation rather than an increase in the number of cell layers (Smith and Schoenwolf, 1987; Smith and Schoenwolf, 1988). The process of neural plate development and morphogenesis also requires an inductive signal, sonic hedgehog (SH), produced from the underlying notochord (Smith and Schoenwolf, 1989).

Shaping of the neural plate, driven by changes in the neuroepithelial cell behavior, results in mediolateral narrowing and rostrocaudal elongation. On a cellular level, shaping involves thickening, narrowing and lengthening of the neural plate driven by neuroepithelial cell elongation (Schoenwolf and Alvarez, 1989). About half the daughter cells produced during neurulation are destined to lengthen the neural plate rather than widen it (Sausedo *et al.*, 1997).

Bending, which is initiated during neural plate development, results in the formation of the neural folds and subsequent elevation and convergence of the neural

folds toward the dorsal midline. This occurs in two steps, furrowing and folding (Schoenwolf and Franks, 1984). Bending of the neural plate is driven by changes in both neuroepithelial cells (intrinsic forces) and the adjacent cells of the epidermal ectoderm (extrinsic) (Schoenwolf, 1988; Moury and Schoenwolf, 1995). Wedging of neuroepithelial cells is driven by changes in cell shape within the neural plate (Schoenwolf and Smith, 1990), which causes furrowing, whereas folding of the neural plate largely depends on extrinsic changes, which leads to the expansion of epidermal ectoderm (Lawson *et al.*, 2001).

Development and extension of the neural folds allows the pair of neural folds to contact and fuse at the dorsal midline establishing the roof of the neural tube (Smith and Schoenwolf, 1991). The neural tube then separates from the overlying epidermal ectoderm. As a result, two separate epithelial layers are formed; epidermal ectoderm and neuroepithelium with intervening neural crest cells. The neural crest cells arise during the formation of the neural folds and are largely involved in the formation of the peripheral nervous system. (Anderson, 1999; Castro and Bronner-Fraser, 1999; Groves and Bronner-Fraser, 1999; Hall, 1999; Le Douarin and Kalcheim, 1999).

### ***Neurulation, Neural Tube Defects and Folate Deficiency***

Neural tube defects (NTDs) are the most common birth defects in the United States (Copp *et al.*, 1990; Desesso *et al.*, 1999; Harrist and Juriloff, 1999). Therefore it is safe to assume that NTDs have both genetic and environmental bases. 50%-66% of these incidents can be prevented with folic acid supplementation during early pregnancy



(Czeizel and Dudas, 1992). Although the reasons for such preventions are unclear (Luccock and Deskalakia, 2000), it is evident that neurulation genes are involved. Neurulation genes are those that regulate and coordinate unique combinations of cell behaviors in tissues involved in neurulation. 28 genes have been identified as required for normal neurulation (reviewed by Colas and Schoenwolf, 2001). These include genes that are involved in regulation of other genes (*Cart-1*, *c-ski*, *jmj*, *kappa*, *RBP-J*, *Pax3*, *Tcfap2a* and *twist*), cell adhesion or its regulation (*Calr*, *Efna5*, *Fkbp1a*, *Itga3+Itga6*, *Lama5* and *Pig-a*), regulation of cytoskeletal dynamics (*Enah*, *Macs*, *Mlp*, *RhoGAP5*, *shrm*, *abl+arg* and *Vcl*), nutrition of embryo (*apoB* and *Folbp1*) and other various functions (*Bcl10*, *Csk*, *Ikk1+Ikk2*, *Juk1+Jnk2*, *Psen1+Psen2* and *terc*) (Colas and Schoenwolf, 2001). Relevant to this study are *Pax-3* (a transcription factor involved in neurogenesis), *twist* (transcription factor expressed in neural crest) and *Folbp1* (folate acid binding protein 1).

Embryonic and fetal cells depend entirely on maternal sources of folate during gestation. In mice, a 50% reduction of maternal liver folate was associated with a threefold increase in the percentage of the litter affected by cleft palate (Sakanashi *et al.*, 1996). It was found that when placental development was impaired by folate deficiency, the babies were small. Folate insufficiency later in pregnancy resulted in subtle birth defects associated with neuroepithelial and neural crest cell derived structures including, neural tube, parts of the eye and craniofacial structures (Colas and Schoenwolf, 2001).

Homozygosity for a variant of 5,10-methylenetetrahydrofolate reductase (MTHFR), a folate pathway enzyme (Figure 1), is a genetic risk factor that results in

about 15% of NTDs (Van der Put *et al.*, 1997). A study done using folate receptor (FR) knock-out and knock-down mice resulted in a high percentage of folate responsive NTDs (Antony and Hansen, 2000). In the same study they found folate deficiency led to the up-regulation of FRs, which implies a critical role played by FRs in folate homeostasis (Antony and Hansen, 2000). An upregulation of FRs due to low levels of folate resulted in reduced cell proliferation. Also, it was apparent that FRs are expressed in both placental and embryonic tissues and play a critical role in folate uptake by the embryo (Hansen *et al.*, 1999). Therefore, low levels of folate increase the presence of FRs in embryonic and placental tissues as well as decrease cell proliferation. Such a reduction in cell proliferation of either placental, neural tube or neural crest cells could result in serious consequences to the embryo (Antony and Hansen, 2000).

The metabolite homocysteine, which increases during folate deficiency (Allen *et al.*, 1993) has been identified as a risk factor for NTDs (Steegers Theunissen *et al.*, 1994; Van Aerts *et al.*, 1994) and placental abruption (Wouters *et al.*, 1993). Homocysteine synthesis is dependent on the metabolite SAM (Figure 1). Increased homocysteine has been shown to be associated with folate-responsive congenital heart defects and NTDs (Rosenquist *et al.*, 1996). The cellular accumulation of homocysteine also increases the upregulation of FRs (Sun and Antony, 1996).

*Pax-3* is expressed in closing neural folds and adjacent tissues. Although *Pax-3* mutations do not appear to be the cause of most of the NTDs seen in humans, misregulation of the *Pax-3* transcription factor which may regulate genes such as *N-CAM*, *N-cadherin*, *c-met*, *MyoD*, *Myf-5* and *versican* could be involved in some cases of

NTDs. Studies on homozygous *plotch* (*Pax-3*) knock-outs have demonstrated a folate-responsive NTD (Fleming and Copp, 1998). These NTDs seen in *plotch* *-/-* embryos are rescued by folic acid. Interestingly these NTDs can also be rescued by thymidine. Deoxythymidine monophosphate (dTMP) can be synthesized from deoxyuridine monophosphate (dUMP) or thymidine. Normally, incorporation of [3H]thymidine into dTMP is suppressed by exogenous dUMP. In homozygous *plotch* *-/-* mice the abnormal suppression of deoxyuridine leads to the development of anencephaly and spina bifida. These homozygous mutants incorporate significantly more [3H]thymidine into dTMP in the absence of dUMP compared to the wild type. Administering folic acid or thymidine to the embryo lowers the [3H]thymidine incorporation and prevents the development of some NTDs. This demonstrates that cell specific defects can influence the embryological process in adjacent tissues, affecting the entire cascade of development (Fleming and Copp, 1998).

A systematic approach of looking at expression patterns of genes, which also includes genes that are other than those folate related, is required to identify neurulation genes that might better explain the incidence of NTDs (Stumpo *et al.*, 1998; Melvin *et al.*, 2000; Joosten *et al.*, 2001). The expression of these genes may be influenced by folate levels in the mother and consequently the growing embryo.

### ***Folate Deficiency and Effects on Gene Expression during Development***

The relationship between folate status and increased risk of neural tube defects such as spina bifida is well established (Lucock, 2000). The molecular mechanism by

which folate status influences neural tube closure and other developmental events has not been clearly determined. It has been hypothesized that the relationship between folate and developmental defects is a reduction in cell division, particularly within rapidly dividing cell populations of the embryo (Antony and Hansen, 2000). Surprisingly, there are limited data supporting this idea and in some studies, no change in cell numbers were detected (Barbera *et al.*, 2002). As reviewed in the previous section, folate deficiency has been shown to contribute to NTDs. There is also evidence that folate deficiency leads to specific changes in gene expression. It has been proposed that these changes contribute to developmental defects (Barbera *et al.*, 2002; Tang *et al.*, 2003; Lucock *et al.*, 2000; Duthie, 1999; Olshan *et al.*, 2005).

The consequences of reduced folate in development and gene expression were analyzed in a mouse with a knockout of the folic acid-binding protein 1 (*Folbp1*) gene (Tang *et al.*, 2003). *Folbp1* is a membrane protein with a high affinity for folic acid. *Folbp1* nullizygous embryos lose the ability to transport folic acid into the epithelial cells. In this study, expression patterns of the crucial genes such as *Pax-3*, *En-2*, *Hox-a1*, *Shh*, and *Wnt-1* were examined. Inactivating *Folbp1* in mice was embryonic lethal with severe cranial neural tube and oro-facial defects. The neural tube failed to fuse and the mid and hindbrain remained widely open. Nullizygous *Folbp1* embryos were rescued by supplementing the diet of the pregnant heterozygous females with folic acid, indicating that *Folbp1* and folate are essential for proper embryogenesis.

*Pax-3* is normally expressed from midbrain region down the entire length of the neural tube in wild type embryos. This expression was almost absent in *Folbp1*

nullizygotes embryos. *En-2*, essential for development of midbrain and cerebellum, is highly expressed in the midbrain-hindbrain region of the wild type and this expression was significantly reduced in the *Folbp1* knockout embryos and was restricted to the hindbrain region. There was no significant difference in the expression patterns of *Hox-a1* and *Wnt-1* in either the wild type or nullizygous embryos. The normal expression pattern of *Shh* in the neural tube from the level of the forebrain, going posterior, expanded extensively with a high level of expression in the midbrain region of the *Folbp1* *-/-* mice. These results suggest that folate deficiency is altering the expression of genes required for proper cell proliferation and differentiation (Tang *et al.*, 2003).

In another genetic study, *Cited2* deficient mice were used to test the ability of folate to reduce exencephaly (Barbera *et al.*, 2002). Anencephaly, a condition with many of the same underlying causes as exencephaly is seen in births associated with folate deficiency. *Cited* genes encode nuclear proteins that bind to transcriptional co-activators and enhance transcription. *Cited2**-/-* mutant mice die before birth and exhibited heart defects and exencephaly. It was found that *Cited2* was required for the survival of neuroepithelial cells and its absence led to massive apoptosis in dorsal neuroectoderm around the forebrain-midbrain boundary and in a restricted domain in the hindbrain. When *Cited2**+/-* pregnant females were treated daily with folic acid, the exencephaly was reduced from 80% to 12.5% in the *Cited2**-/-* embryos analyzed at 14.5 days post coitum. The same type of effect was observed using embryos cultured *in vitro* and treated with folic acid for 24 hours. Considering that *Cited2**-/-* mutants revealed no defects in folate metabolism, folic acid does not compensate for an intrinsic defect of folate metabolism in

the embryos and they observed no reduction in the level of apoptosis or increased cell proliferation in *Cited2*<sup>-/-</sup> embryos treated with folic acid. This led to the idea that folic acid can decrease the incidence of NTDs by a mechanism other than compensating for a folate related defect in the embryos (Barbera *et al.*, 2002).

Decreased levels of folate result in elevated levels of homocysteine, which is associated with neural tube defects (Afman *et al.*, 2003). Neuroepithelial cells, cranial neural crest cells and cardiac neural crest cells are involved in neural tube defects, orofacial defects and conotruncal heart defects, respectively (Kirby *et al.*, 1985; Poelmann *et al.*, 1998; Botto *et al.*, 1999). Folate receptors are highly expressed in the cells of neurectoderm, which are precursor cells of both neural crest and neuroepithelial cells. This could explain why the beneficial effect of folic acid is specific for neuroepithelial and neural crest cells (Boot *et al.*, 2003). A study performed to examine behavior of neuroepithelial cells in the presence of increased concentrations of folate and homocysteine resulted in increased outgrowth and migration of neural crest cell from the neural tube and inhibition of neural crest cell differentiation in the presence of homocysteine. Addition of folic acid led to increased outgrowth of neuroepithelial cells and neural crest cell differentiation into nerve and smooth muscle cells. This suggests that NTDs caused by folate deficiency and hyperhomocysteinemia is due to increased neuroepithelial to neural crest cell transformation, leading to a lower number of neuroepithelial cells in the neural tube and a failure to close the neural tube (Boot *et al.*, 2003). More generally, it indicates that folate deficiency can alter cellular differentiation.

## ***Research Overview***

Approximately 1 out of every 2000 births are effected by defects directly related to the abnormal development of the brain, spinal chord or the improper development of structures (heart, peripheral nervous system, skeletal and connective tissues and endocrine tissues) derived from the neural crest cells (Wilt and Hake, 2004; Northrup and Volcik, 2000). Many studies have shown that administering the B vitamin, folate, to the pregnant mother reduces the prevalence of NTDs by as much as 48% (Daly *et al.*, 1995). Numerous genes important in the regulation of neurulation have been identified that could be involved in NTDs (Colas and Schoenwolf, 2001). Although it has been established that folate reduce NTDs, the underlying mechanism is unclear. Therefore, a systematic approach based on expression patterns of genes is required to understand the mechanisms underlying folate-related birth defects involving the neural tube. The hypothesis guiding this project is that the developmental defects associated with folate deficiency are due to changes in gene expression. In order to investigate this hypothesis two specific aims need to be considered:

1. determine if methotrexate and homocysteine treatment of *Xenopus* embryos can lead to developmental (neural tube and gross morphological) alterations associated with folate deficiency.
2. analyze the spatial expression pattern of specific genes in *Xenopus* embryos with altered folate metabolism and *Xenopus* embryos cultured in conditions that mimic altered folate metabolism.

## CHAPTER II

### MATERIALS AND METHODS

#### *Embryo Culture*

*Xenopus laevis* embryos prepared by *in vitro* fertilization and cultured in the laboratory (Newport and Kirschner, 1982) were used in this study. Adult *Xenopus laevis* were ordered from Xenopus I (Dexter, MI). Testis tissue was removed from male frogs and cultured in oocyte culture medium [OCM: 50% Leibovitz, medium containing 15mM N-2-hydroxyethylpiperanziner-N'-2-ethanesulfonic acid (HEPES), pH 7.8, 1 mM 1-glutamine, 0.4 mg/ml bovine serum albumin, 1 µg/ml bovine pancreatic insulin, 100 µg/ml gentamicin sulphate, 50 U/ml nystatin]. Female frogs were injected with 600 U of human chorionic gonadotropin (Sigma Chemical, CAT#CG-10, St. Lewis, MO) eight hours before *in vitro* fertilization to stimulate ovulation. Eggs were stripped manually from the female frogs and put in a Petri dish. Testis tissue was placed next to eggs, smashed, and suspended in 1X Modified Barth's Saline [MBS: 88 mM NaCl, 1 mM KCl, 2.4 mM NaHCO<sub>3</sub>, 0.82 mM MgSO<sub>4</sub>•7H<sub>2</sub>O, 0.33 mM Ca(NO<sub>3</sub>)<sub>2</sub>•4H<sub>2</sub>O, 0.41 mM CaCl<sub>2</sub>•6H<sub>2</sub>O] to activate the sperm. The sperm suspension was placed onto the egg clutch and allowed to sit for two minutes. Fertilization was initiated by adding deionized water to eggs and testis. About 20 minutes later, when cortical rotation had occurred, water was replaced by 2% cysteine-HCl solution (4 g of cysteine in 200 ml of H<sub>2</sub>O, pH 7.8 with 12N NaOH) to remove the jelly coat that holds the eggs together. Following the removal



of jelly coats, the embryos were rinsed with water and cultured in 0.1X MBS at room temperature. The developmental stages were determined according to Nieuwkoop and Faber (1967).

As the embryos went through the first stages of cell division the most normal appearing embryos were selected by visual examination and transferred to a new culture dish. About 4 hours after fertilization at stage 7, the embryos were transferred into 0.1X MBS containing different concentrations of methotrexate and homocysteine.

### ***Preparation of compounds***

To prepare 40 ml of 300  $\mu$ M methotrexate in 0.1X MBS; 5.4 mg of methotrexate (Sigma, CAT# M-9929 or Fluka, CAT# 59-05-2) was added to 2 ml of water and titrated with 5N NaOH (approximately 5  $\mu$ l) until the methotrexate dissolved. To this 2 ml solution of methotrexate, 4 ml of 1X MBS along with 34 ml of water was added to bring the volume up to 40 ml. Using this stock solution, dilutions were made with 0.1x MBS to the final concentrations of 1  $\mu$ M, 10  $\mu$ M, 50  $\mu$ M, 100  $\mu$ M and 200  $\mu$ M.

Stock of 370 mM concentrations of homocysteine was prepared by mixing 0.75 g of homocysteine (Sigma, CAT# H-4628) with 15 ml of 0.1N HCl. To prepare 40 ml of 100 mM homocysteine, 10.8 ml of homocysteine stock solution was mixed with 4 ml of 1X MBS and 25.2 ml of water. The 100 mM stock was adjusted to pH 7.2 using 1N NaOH and diluted with 0.1X MBS to prepare 0.5 mM, 1 mM, 10 mM, 25 mM and 50 mM.

### ***Analysis of Gross morphology, Gut Coiling and Neural Tube Thickness***

*Gross Morphology:* Throughout development of the treated and untreated embryos, gross morphological effects were analyzed including tail length and shape, size of eyes, head shape and size and the presence of structural abnormalities in the gut.

*Gut Coiling:* At stage 45 (tadpole), about 4 days and 2 hours past fertilization (hpf.), embryos were fixed with 4% paraformaldehyde for 1-2 hours at room temperature and dehydrated in 100% ethanol (EtOH) to examine the direction of gut coiling under light microscopy. The embryos were categorized according to left coiled, right coiled or deformed as described in the results section.

*Neural Tube Thickness:* At stage 27 (30 hpf.) the embryos were fixed, sectioned and stained to examine the neural tube, as described below.

### ***Embryo Fixation, Embedding and Sectioning***

*Infiltration and Embedding of Embryos:* Embryos were fixed with 4% paraformaldehyde and dehydrated using an EtOH/0.1 X MBS series (25%, 50%, 75% and 100% EtOH). Half the ethanol was replaced with Hemo-De for 5 minutes at room temperature prior to replacing the ethanol/Hemo-De mixture twice with fresh Hemo-De (CAT # 15 182 507A, Fisher) at 10 minute intervals. Then, half the Hemo-De was replaced with molten paraplast (CAT # P3683, Sigma) and incubated for 10 minutes at 55° C before replacing the Hemo-De/ paraplast mixture with fresh paraplast and incubating at 55° C for 1 hr. The paraplast was replaced twice at 30 minute intervals and embryos were incubated at 55° C. Finally, the paraplast was replaced and incubated over

night at 55° C. The infiltrated embryos were positioned into a mold and were embedded in paraplast, which were allowed to harden over night at room temperature.

*Slide Preparation and Subbing for Paraplast Sections:* Slides were cleaned individually with 95% EtOH and a Kimwipe and soaked in 70% EtOH for 1-2 hours. The slide edges were blotted with a clean absorbent surface before dipping in subbing solution (0.01% of chromium potassium sulfate added to 0.1% of gelatin in water). When the slides were evenly coated they were tented with aluminum foil and allowed to dry.

*Sectioning and Processing of Embryos:* The embryos were sectioned at 11 micrometers on a microtome (Microm HM 315) and the sections were moved onto slides coated with subbing solution. The sections were allowed to dry so the sections adhered to the slide and washed twice in Hemo-De for 3 minutes at room temperature to remove the paraplast from sections. The sections were hydrated using an EtOH series (100%, 75%, 50% and 25% EtOH), stained with Harris Haematoxylin for about 3 minutes, rinsed with running water for 60 seconds and neutralized in alkaline alcohol (35% EtOH with a pinch of sodium bicarbonate) for 1 minute. The sections were dehydrated using 70% EtOH, counter stained with eosin in 70% EtOH for 3 minutes and the excess stain was rinsed away with 70% EtOH. The sections were dehydrated again using an EtOH series, washed in Hemo-D for 2 minutes before adding a drop of mounting resin and placing a cover slip.

*Analyzing the sections:* The sections were observed under light microscopy and digitally photographed using a Cannon DS 6031 camera. The thickness of the dorsal,

ventral and mediolateral ends of the neural tube was measured from the printed photographs.






### ***Analysis of Gene Expression by Whole-mount In situ Hybridization***

Whole-mount *in situ* hybridizations were performed according to Harland (1991) with some modifications.

*Preparation of Embryos:* Right after the jelly coats were removed, albino *Xenopus laevis* embryos were stained with 0.01% Nile blue in 50 mM phosphate buffer, pH 7.8 to help determine the exact developmental stage of embryos. Healthy looking embryos were treated with 1 mM and 10 mM homocysteine and 50  $\mu$ M and 100  $\mu$ M methotrexate in 0.1x MBS. Embryos were collected at stages 12 (gastrula), 20 (neurula) and 26 (tail bud). The vitelline envelopes were removed in some of the stage 20 and stage 26 embryos. Embryos were fixed in fresh MEMFA buffer (0.1 M 3-[N-morpholino] propanesulfonic acid (MOPS), pH 7.4, 2 mM EGTA, 1 mM magnesium sulfate (MgSO<sub>4</sub>), 3.7% formaldehyde) with gentle agitation at room temperature for 1-2 hours. Following fixation, embryos were dehydrated with methanol (MeOH) and stored at -20° C.

*Probe Synthesis:* pBluescript Plasmids containing cDNAs coding for *Xenopus Dkk-1* (pRNDkk-1), *Wnt-5A* (pBSXE3), *Pax-3* (Pax3 D2), *Xbra* (pXbrachyury) and *Xtwist* (pXtwist) were linearized with appropriate restriction enzymes such that sense and anti-sense transcripts can be generated using T3, T7 or Sp6 RNA polymerase as appropriate (Table 1).

**Table 1.** Characteristics of Genes used for *In situ* Hybridization Studies.

Gene Name	Function	Expression Pattern	Plasmid Name	Riboprobe <sup>1</sup>		Reference
				Sense	Anti-sense	
Pax-3	A member of the paired box (PAX) family of transcription factors, which play critical roles during neurogenesis.		Pax3 D2	Not I (Sp6)	Sal I (T3)	Bang et al., 1999; Monsoro-Burq et al., 2005
Wnt5A	A member of the WNT gene family which encodes secreted signaling proteins. <i>Wnt5A</i> signaling mediates axis induction.		pBSXE3	EcoR I (T7)	Kpn I (T3)	Moon et al., 1993
Dkk-1	A member of a family that encodes secreted proteins. <i>Dkk-1</i> is a antagonist of the Spemann organizer and is required for head formations.		pRNDkk-1	Kpn I (T3)	Hind III (T7)	Monaghan et al., 1999; Kazanskaya et al., 2000; Glinka et al., 1998
XBra	A mesodermal transcription factor. Controls the early Hox expression domain in the animal-vegetal direction		pXbrachyury		EcoR V (T7)	Smith et al., 1991
XTwist	A transcription factor expressed in the neural crest		pXTwist		Kpn I (T7)	Hopwood et al., 1989

<sup>1</sup> Enzymes used to linearized plasmid for probe synthesis

The volume of the digested DNA sample was increased up to 100  $\mu$ l with diethylpyrocarbonate (DEPC) treated H<sub>2</sub>O. To the above mixture, an equal volume of phenol chloroform was added, vortexed and spun for 5 min at 16000 x g. Then, the supernatant was transferred to a new tube and an equal volume of chloroform was added to the supernatant. The mixture was centrifuged again for 5 min at 16000 X g and supernatant was removed to a clean tube. 0.1X volume of 3M NaAcetate and 2X volume of absolute EtOH was added to the supernatant and the mixture was vortexed before placing it at -20° C overnight. The next day, the DNA mixture was centrifuged for 10 min at 16000 X g, EtOH removed, 100  $\mu$ l of 70% cold EtOH was added and centrifuged for 5 min at 16000 X g. The supernatant was removed and the DNA pellet was air dried prior to resuspending in 20  $\mu$ l of DEPC ddH<sub>2</sub>O. In order to synthesize the RNA probe, 2.5  $\mu$ g of linearized template DNA was added to a mixture containing 1X transcription buffer, 10 mM DTT, 1% RNAsin, 60 units of the appropriate RNA polymerase, rNTP mix [2.5 mM CTP, GTP, ATP, 1.6 mM UTP and 0.9 mM digoxigenin (dig) -UTP (Boehringer-Mannheim Biochemical, CAT# 209256)] and DEPC treated H<sub>2</sub>O. The reaction was incubated at 37° C for 2 hrs and DNase was added to each sample to eliminate template DNA. The samples were centrifuged through a G-50 spin column to remove unincorporated nucleotides from the synthesized RNA (Eppendorf-5 Prime, CAT# 3-337047, Boulder, CO). To the RNA sample, 0.1X volume of 3 M NaAcetate with 2.5X volume of 100% EtOH was added and the sample was stored at -80° C overnight or longer. The precipitated RNA was pelleted by centrifuging the sample at 4° C, 16 000 X g for 10 min. The supernatant was removed, 500  $\mu$ l of 70% EtOH was added

to the RNA pellet and the sample was centrifuged for 5 min at 40 000 xg. The sample was air dried and resuspended in 200 µl of hybridization buffer [0.1% CHAPS, 1X Denhart's, 5 mM EDTA, 50% formamide, 100 µg/ml Heparin, 5X sodium citrate (SSC), 0.5 mg/ml *Torula* RNA, 0.1% Tween-20 and DEPC treated H<sub>2</sub>O. The probe stocks were stored at -80° C until use.

*Hybridization of Embryos with RNA Probes:* 0.5 volume of DEPC H<sub>2</sub>O was added every 5 minutes to the embryos stored in 100% MeOH until the MeOH concentration reached 25%. The embryos were then washed thoroughly with PBST [1X phosphate-buffered saline (PBS) and 0.1% Tween-20] five times for 5 minutes each time. The embryos that had been fixed with the vitelline membrane intact (stage 12) were incubated in proteinase K (10 µg/ml), collagenase A [2 mg/ml (Roche, CAT# 103 578)] and hyaluronidase [20 U/ml (Sigma, CAT# H-4272)] for 10 minutes at room temperature to remove the vitelline membrane and to permeabilize the embryos. Embryos that had hatched or with removed vitelline membrane were incubated in proteinase K at room temperature for 15 minutes. Embryos were then washed in PBST three times for 5 minutes to remove the proteinase K, followed by two 5 minute washes in 0.1 M Triethanolamine (TEA). In order to prevent electrostatic interactions between probe and basic proteins, 10 µl of acetic acid anhydride was added twice, at 5 minute intervals to each vial containing 4 mls of 0.1 M TEA. Following neutralization, the embryos were washed twice in PBST, refixed in 4% paraformaldehyde in PBST for 20 minutes, washed 5 times in PBST and transferred into 20 % hybridization buffer/80% PBST. These embryos were pre-hybridized over night at 60° C in hybridization buffer. The next day, 1

ml of hybridization buffer containing ~2 µg of probe was added to each vial and embryos were incubated over night at 60° C. Prior to adding Dig-labeled RNA probes, the probe/hybridization buffer mixture was incubated at 75° C for 5 minutes to denature the probe. Following hybridization, the probe was removed and stored at -80° C to be re-used. The embryos were washed with hybridization buffer for 10 minutes at 60° C, followed by four 20 minute washes in 2X sodium citrate (SSC) (20X SSC: 3 M NaCl and 0.3 M Na citrate, pH to 7.6 with HCl) and a high-stringency wash for 1 hr in 0.2X SSC at 60° C. Then, the embryos were incubated in a 1X maleic acid buffer (MAB) (5X MAB: 0.5 M maleinic acid and 0.75 M NaCl), pH 7.5, containing 2% Boehringer-Mannheim Blocking Reagent (BMBR) (Roche, CAT# 1096176) at room temperature followed by two consecutive 15 minute washes in 1X MAB at 60° C and room temperature. Next, the embryos were blocked for 1 hr at room temperature in 0.9 ml of blocking buffer lacking antibody (MAB containing 20% heat inactivated lamb serum and 2 % BMBR). The blocking buffer was removed and replaced with 0.1 ml of blocking buffer containing anti-dig antibody (Boehringer-Mannheim Biochemical, CAT# 1093274, Germany) diluted 1:2000 and incubated overnight at 4° C. The next day, the embryos were thoroughly washed with four 1 hr washes at room temperature in 1X MAB and then incubated in 1X MAB overnight at 4° C. The embryos were equilibrated with two 5 minute washes in alkaline phosphatase (AP) buffer [100 mM Tris (pH 9.5), 50 mM MgCl<sub>2</sub>, 100 mM NaCl, 0.1% Tween-20 and 5 mM Levamisol] at room temperature before adding 1 ml of BM Purple AP substrate (Roche, CAT# 1442074) to start the color reaction. The staining reaction was kept in dark for 5-6 hrs at room temperature to



achieve the proper level of staining. The stained embryos were washed thrice with 1X PBS for 5 minutes at room temperature. The color reaction was stopped by two 30 minute washes at room temperature in MEMFA. The embryos were then dehydrated in methanol and examined under bright field microscopy. The images were captured using a Olympus PM-C35DY and processed using Adobe Photoshop 7.0. Some embryos were bleached to reduce the background staining by incubating overnight at 4° C in 2:1 MeOH/H<sub>2</sub>O<sub>2</sub> under high light. Also, some embryos were cleared to allow for examination of internal staining in 1:2 Benzyl Alcohol/Benzyl Benzoate (BA/BB) solution until the embryos sank to the bottom of the vial.

## CHAPTER III

### RESULTS

#### *Development of Embryos Treated with Homocysteine and Methotrexate*

The *Xenopus* embryo is an ideal system to investigate the link between the effects of folate deficiency and associated developmental defects because the embryos are readily available and there is extensive knowledge of the morphological and molecular details of development. One problem, however, is the inability to deplete the folate naturally present in the egg and available to the growing embryo. As an alternative, I chose to simulate effects of altered folate metabolism by treating growing embryos with methotrexate and homocysteine. Methotrexate inhibits an enzyme in the folate pathway, dihydrofolate reductase (Figure 1). Consequently, the central folate pathway is blocked leading to a reduction in 5, 10, methylene-THF and 5-methyl-THF, the folate intermediates required for deoxythymidine monophosphate (dTMP) and methionine biosynthesis, respectively. Homocysteine is a naturally occurring amino acid that is methylated to produce methionine. When 5- methyl-THF is not generated there is a decreased conversion of homocysteine to methionine and corresponding increase in homocysteine. Thus, addition of homocysteine is expected to mimic, in part, folate deficiency in the embryo.

For these initial studies we examined the gross morphology (overall development, size of the head, length of the body, size of the eyes and direction of gut coiling) and

neural tube of homocysteine and methotrexate treated embryos. Methotrexate treatment has also been shown to result in randomization of the direction of gut coiling in *Xenopus* embryos (Bantle *et al.*, 1990). Therefore, direction of gut coiling was categorized in *Xenopus* embryos that had been grown in different concentrations of methotrexate and homocysteine. A similar effect on gut coiling would suggest a suitable concentration of methotrexate and homocysteine to use in these studies and also that homocysteine and methotrexate lead to a similar morphological end point.

### ***Xenopus Development and Gross Morphological Defects***

#### ***Homocysteine***

*Xenopus* embryos were grown in different concentrations (0.5 mM, 1 mM, 10 mM, 25 mM, 50 mM and 100 mM) of homocysteine and their gross morphology was compared (Figure 2). No difference in development or morphology was observed up to gastrula stage (stage 12). Embryos treated with 100 mM homocysteine did not develop beyond the gastrula stage. By stage 23, some embryos treated with 10 mM homocysteine were underdeveloped compared to the controls. By stage 41 it was evident that the embryos treated with 10 mM and 50 mM were exhibiting developmental defects, such as kinked bodies, underdeveloped guts, small eyes or were generally deformed compared to untreated embryos. However, at concentrations of 10 mM and above, there were some embryos that exhibited normal development within the same group of embryos. At stage 45 (tadpole stage) the developmental defects in embryos treated with 10 mM and 50 mM

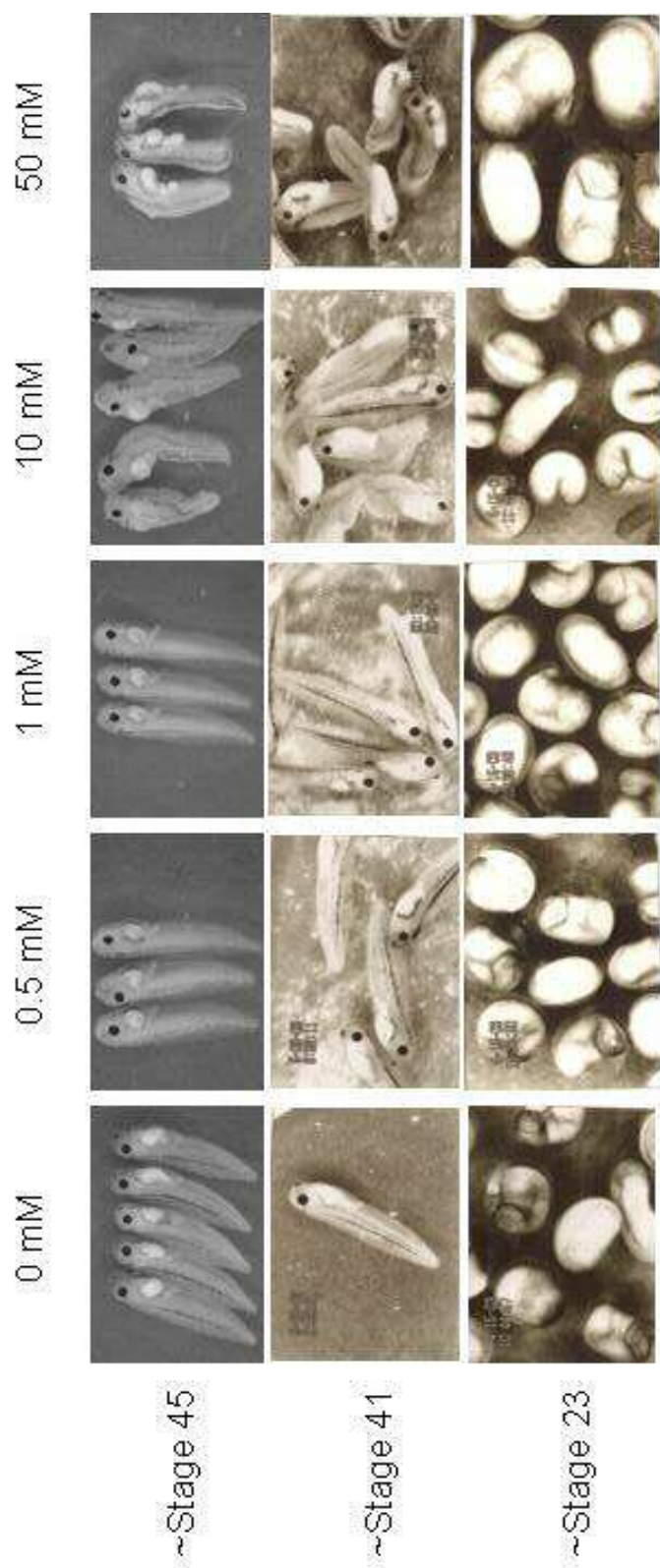


**Figure 2. Development of *Xenopus* Embryos Treated with Homocysteine.** Fertilized eggs were allowed to develop to stage 7 (~ 4 hpf) and transferred into 0.1 x MBS, containing the indicated amounts of homocysteine. Embryos treated with 100 mM homocysteine did not survive beyond gastrulation

were obvious with smaller and kinked bodies and deformed internal structures. In particular, the guts were severely deformed or miscoiled.

### *Methotrexate*

*Xenopus* embryos were grown in different concentrations (1  $\mu$ M, 10  $\mu$ M, 50  $\mu$ M, 100  $\mu$ M and 200  $\mu$ M) of methotrexate and their gross morphology was compared (Figure 3). By the time control embryos reach stage 26, 1  $\mu$ M, 10  $\mu$ M and 50  $\mu$ M methotrexate treated embryos included individuals with different developmental stages, ranging from stage 24-26. At 100  $\mu$ M, the developmental stages of the embryos varied from stages 12-26 and some of the embryos did not survive beyond stage 12 (gastrula). In each set of treated embryos, there were embryos with deformities such as small eyes, deformed and kinked bodies and underdeveloped or missed coiled guts. Although the severity of the deformities increased as the methotrexate concentration increased, some of the embryos even above 100  $\mu$ M showed normal development.

### *Survival and Direction of Gut Coiling*

The embryonic gut is derived from the endodermal germ layer. Development of *Xenopus laevis* gut starts 3 days past fertilization (Chalmers and Slack, 1998; Chalmers and Slack, 2000). Previous studies have shown that randomization of gut coiling occurred due to teratogens (Bantle *et al.*, 1990; Vismara *et al.*, 2000) and changes in gene expression (Branford *et al.*, 2000). In particular, adding methotrexate has resulted in randomization of the *Xenopus* gut along with defects such as microphthalmia,

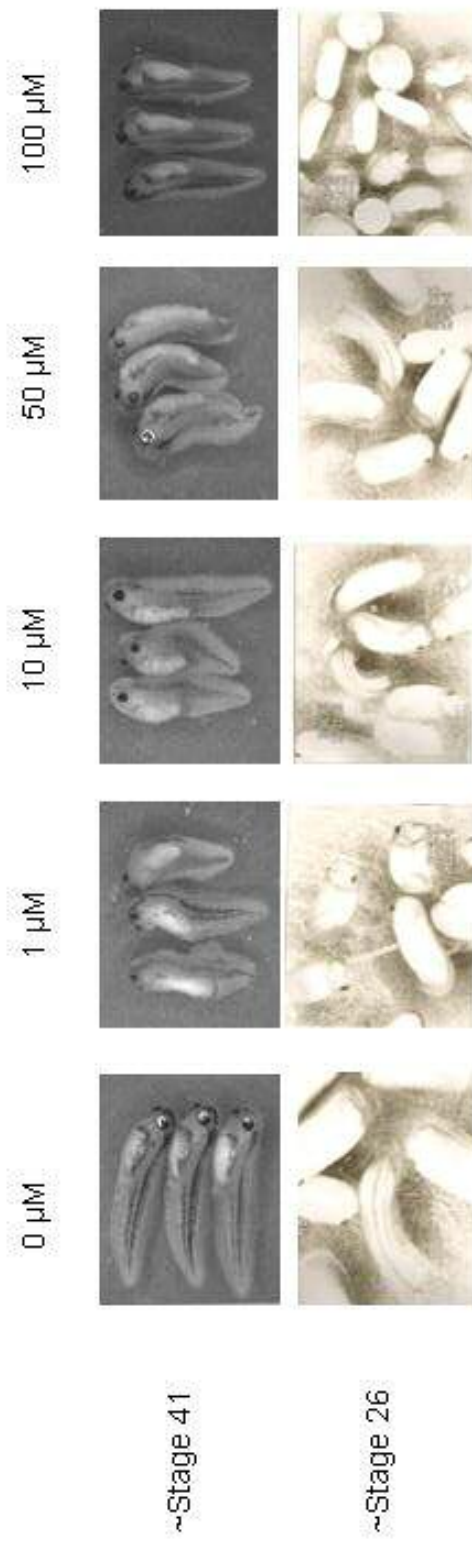


**Figure 3. Development of *Xenopus* Embryos Treated with Methotrexate.** Fertilized eggs were allowed to develop to stage 7 (~ 4 hpf) and transferred into 0.1 x MBS, containing the indicated amounts of methotrexate.

micoencephaly and hydroencephaly, in neuroepithelial derived structures (Bantle *et al.*, 1990). Therefore, during this study I looked at direction of gut coiling in embryos treated with homocysteine and methotrexate to establish concentrations that is able to cause a detectable effect without killing or severely deforming the embryos.

### *Homocysteine*

In conjunction with this study, I recorded general morphology, survival and the direction of gut coiling of treated and untreated embryos at stage 45. Table 2 is a combination of those data from two separate experiments. Percent mortality for embryos treated with 0.5 mM, 1 mM, 10 mM and 50 mM homocysteine remained between 12%-15%, while untreated embryos had a percent mortality of 7%. In contrast, embryos treated with 100 mM homocysteine did not survive past gastrula stage with a percent survival of 0%. An embryo with two heads was observed at 0.5 mM concentration. At 10 mM homocysteine, live embryos without a gut and an embryo that did not show any structural development was observed. It was evident that the severity of the deformities increased with the increased homocysteine concentrations.

The data for percent coiling to the left and right and percent of embryos with deformed or miscoiled guts are shown in figure 4. Examples of embryos with left, right and miscoiled guts are shown in figure 5. In this experiment, the majority of the guts were coiled to the left in the untreated embryos (Figure 4). As the concentration of homocysteine increased the guts coiling to the left decreased, the number of deformed or miscoiled increased and there was a net increase in the number of guts coiling to the

**Table 2. Survival, General Appearance and Gut Coiling of Homocysteine Treated Embryos.**

<i>Experiment 1</i>				
Concentration of Homocysteine	# of Embryos Survived	# of guts Deformed	# of guts coiled to left	# of guts coiled to right
Control	23	1 (4.3%)	21 (91.3%)	1 (4.3%)
0.5 mM	33	2 (6.1%) 1 underdevel.	26 (78.8%) 1 underdevel.	5 (15.2%)
1 mM	31	4 (12.9%)	23 (74.2%)	4 (12.9%)
10 mM	23	13 (56.5%) 5 no gut	1 (4.3%)	9 (39.1%)
<i>Experiment 2</i>				
Concentration of Homocysteine	# of Embryos Survived (Out of 40)	# of guts Deformed	# of guts coiled to left	# of guts coiled to right
Control 1	38	4 (10.5%)	18 (47.4%) 1 underdevel.	16 (42.1%) 3 underdevel.
Control 2	37	1 (2.7%)	25 (67.6%)	11 (29.7%) 3 underdevel.
0.5 mM 1	30	4 (13.3%) 1 underdevel.	22 (73.3%)	4 (13.3%)
0.5 mM 2	38	4 (10.5%) 1 underdevel. 1 two headed	24 (63.2%)	10 (26.3%) 2 underdevel.
1 mM 1	35	1 (2.9%)	20 (57.1%)	14 (40%) 1 underdevel.
1 mM 2	36	2 (5.6%) 1 underdevel.	26 (72.2%)	8 (22.2%) 2 underdevel.
10 mM 1	36	8 (22.2%) 2 underdevel.	20 (55.6%) 1 underdevel.	9 (25%) 1 underdevel.
10 mM 2	35	22 (62.9%) -1 alive but no cell differentiated	9 (25.7%)	4 (11.4%)
50 mM 1	35	35 (100%)	0 (0%)	0 (0%)
50 mM 2	34	34 (100%)	0 (0%)	0 (0%)
100 mM 1	0	0	0 (0%)	0 (0%)
100 mM 1	0	0	0 (0%)	0 (0%)



For experiment 1, 25-35 embryos were treated with each concentration of homocysteine. During experiment 2, two groups of 40 embryos were treated with 0 mM, 0.5 mM, 1 mM, 10 mM, 50 mM and 100 mM concentration of homocysteine. The embryos were scored at stage 45 (~98 hpf). Underdeveloped (underdevel.) refer to embryos with gut coiling patterns more similar to stages 43 -44 than stage 45.

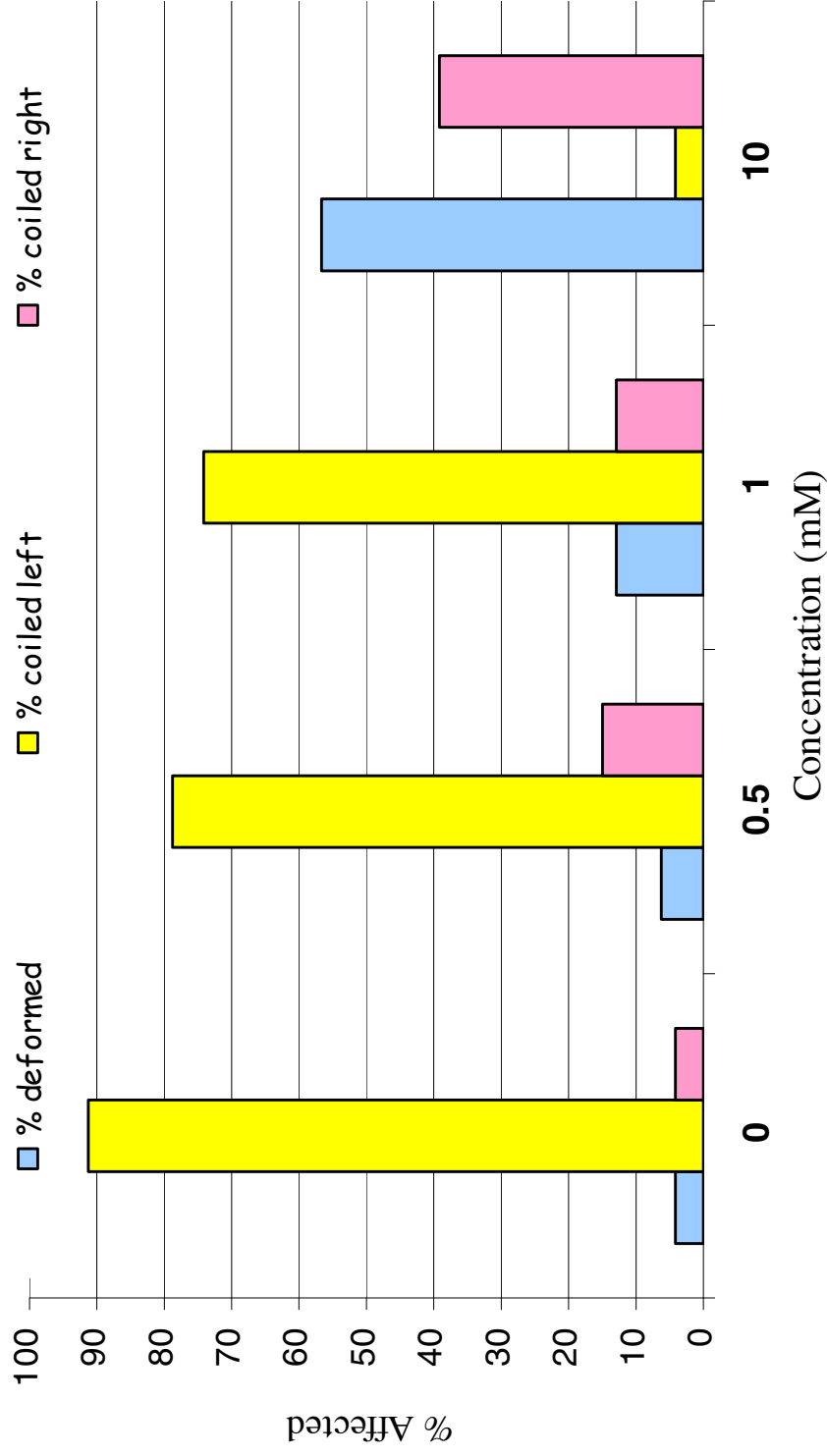


**Figure 4. Direction of Gut Coiling in Embryos Treated with Different Concentrations of Homocysteine .** The embryos treated with different concentrations of homocysteine were fixed at stage 45 (~98 hpf.) and categorized according to the direction or morphology of gut coiling. N= 83 -88.

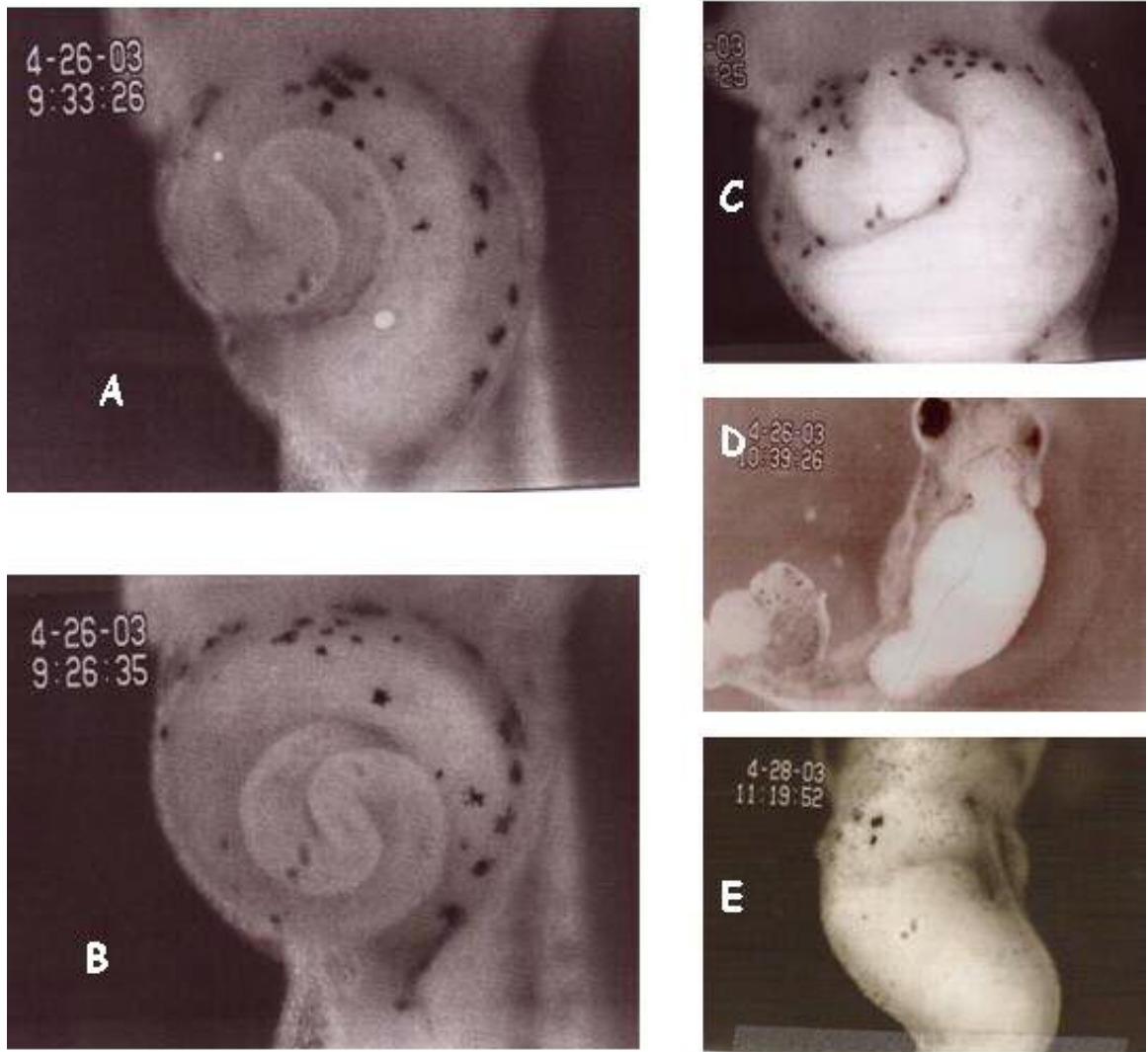


**Figure 5. Examples of Gut Coiling.** Embryos treated with homocysteine and methotrexate were fixed at stage 45 (~98 hpf.) to examine the direction of the gut coiling. The embryos were categorized according to right coiled (A), left coiled (B) and deformed or mis-coiled (C, D and E).

right. At 0 mM ~92 % were left coiled and ~5 % were right coiled. At 10 mM these values were ~5 % and 38 %. There is a substantial increase in the deformed guts and a change in the direction of gut coiling as the concentration of homocysteine increased from 0 mM to 10 mM. All the embryos at 50 mM had deformed guts. The embryos with an underdeveloped gut coiling pattern had a coiling pattern that was more similar to embryos of stage 43 through stage 44 than stage 45.

#### *Methotrexate*

Out of 45 embryos the number of methotrexate treated embryos surviving to stage 45 was determined (Table 3 and Table 4). The percent mortality of embryos treated with 0  $\mu$ M, 1  $\mu$ M, 10  $\mu$ M, 50  $\mu$ M, 100  $\mu$ M and 200  $\mu$ M methotrexate was 1.7%, 8.3%, 3.9%, 4.4%, 8.9% and 4.4%, respectively. Though there is an increase in mortality as the concentration of methotrexate increased, the number of embryos surviving at 1  $\mu$ M was higher than expected. Some embryos within the untreated group were underdeveloped and the number of underdeveloped embryos increased slightly in higher methotrexate concentrations. Also, the number of deformed embryos and the severity of the deformities increased as the concentrations of methotrexate increased. These deformities included kinked bodies, very thin and small bodies and embryos lacking properly defined head structure or trunk structure.

**Table 3. Survival and General Appearance of Methotrexate Treated Embryos.**

<b>Concentration of Methotrexate</b>	<b># of Embryos Survived (Out of 45)</b>	<b># with Significant Morphological Abnormalities</b>
Control 1	45	
Control 2	44	
1 $\mu$ M 1	41	1 very small and deformed and dead. 1 deformed but alive
1 $\mu$ M 2	41	1 deformed but alive
10 $\mu$ M 1	42	1 very kinked and alive 1 severely deformed and barely alive.
10 $\mu$ M 2	44	
50 $\mu$ M 1	44	
50 $\mu$ M 2	42	
100 $\mu$ M 1	40	2 severely badly deformed, but alive
100 $\mu$ M 2	42	2 severely deformed and dead 2 severely deformed but alive, appear to be parts of embryos
200 $\mu$ M 1	44	1 underdev. and dead
200 $\mu$ M 2	42	1 underdev. and dead

Two groups (1 and 2) of 45 embryos each were treated with the indicated concentrations of methotrexate. The embryos were scored at stage 45 (~98 hpf). Underdeveloped (underdev.) refer to embryos that had an overall morphology of a stage earlier than stage 45.

**Table 4. Gut Coiling and the Appearance of Methotrexate Treated Embryos.**

<b>Concentration of Methotrexate</b>	<b>Number of Embryos (Out of 45)</b>	<b>Number of Guts Deformed</b>	<b>Number of Guts Coiled to Left</b>	<b>Number of Guts Coiled to Right</b>
Control 1	45	7 (15.5%) - 2 underdev. - 1 small eyed	28 (62.2%) - 1 very short	10 (22.2%) - 5 underdev.
Control 2	43	7 (16.3%) - 1 coiled inward - 2 underdev.	28 (65.1%) - 2 underdev.	8 (18.6%) - 2 underdev.
1 $\mu$ M 1	42	10 (23.8%) - 2 underdev.	14 (33.3%) - 1 underdev.	18 (42.9%) - 8 underdev.
1 $\mu$ M 2	41	6 (14.6%)	30 (73.2%)	5 (12.2%)
10 $\mu$ M 1	42	12 (28.6%) - 5 underdev.	14 (33.3%) - 4 underdev.	16 (38.1%) - 8 underdev.
10 $\mu$ M 2	45	7 (15.5%) - 2 hardly dev. <sup>1</sup> - 1 no gut formed	22 (48.9%)	16 (35.5%) - 5 underdev.
50 $\mu$ M 1	44	5 (11.4%) - 4 underdev.	24 (54.5%) - 5 underdev.	15 (34.1%) - 5 underdev.
50 $\mu$ M 2	42	3 (7.1%)	38 (90.3%)	11 (26.2%) - 3 underdev.
100 $\mu$ M 1	42	20 (47.6%) - 1 underdev.	15 (35.7%)	7 (16.7%)
100 $\mu$ M 2	44	33 (75%) - 5 underdev.	9 (20.5%) - 8 underdev.	2 (4.5%) - 2 underdev.
200 $\mu$ M 1	44	38 (86.4%) - 7 underdev.	3 (6.8%) - 3 underdev.	3 (6.8%) - 2 underdev.
200 $\mu$ M 2	43	19 (44.2%) - 3 underdev.	15 (34.9%) - 2 underdev.	9 (20.9%) - 3 underdev.

Two groups (1 and 2) of 45 embryos each were treated with the indicated concentrations of methotrexate. The embryos were scored at stage 45 (~98 hpf) according to their gut orientation. Underdeveloped (underdev.) refer to embryos with gut coiling patterns more similar to stages 43-44 than stage 45. In some cases the direction of coiling in underdeveloped embryos could be determined.

<sup>1</sup> dev = developed.

The direction of gut coiling was assessed in embryos cultured in the presence of methotrexate. The data for percent of embryos with deformed or miscoiled guts, guts coiling to the right and the guts coiling to the left are shown in figure 6. The majority of the untreated embryos had guts coiling to the left and there is a net decrease in the number of embryos with guts coiling to the left as the concentration of methotrexate increased with the exception of 50  $\mu$ M. There is also a net increase in the percent of embryos with deformed or miscoiled guts as the concentrations increase with the exception of 50  $\mu$ M. The percent of guts coiling to the right increased from 21% to 37% as the concentration of methotrexate increased from 0  $\mu$ M to 10  $\mu$ M respectively, then decreased to 14% at 200  $\mu$ M. The treated embryos that showed underdeveloped guts had a coiling pattern that was more similar to embryos of stages 43 through stage 44 than stage 45. The decrease seen in right coiling guts could be due to the increase in deformed or mis-coiled guts.

### ***Neural Tube Thickness of Treated Embryos***

It is well known that folate deficiency leads to neural tube defects, such as the failure of neural tube to close properly and anencephaly (Lucock, 2000). On a gross morphological level, we could not detect unclosed neural tubes in homocysteine and methotrexate treated embryos surviving to stage 27. To examine the structure of the neural tube in more detail the neural tube thickness was measured in homocysteine and methotrexate treated embryos. Treated embryos were infiltrated, embedded, sectioned and stained. Sections were examined at the level of first appearance of the ears. Four

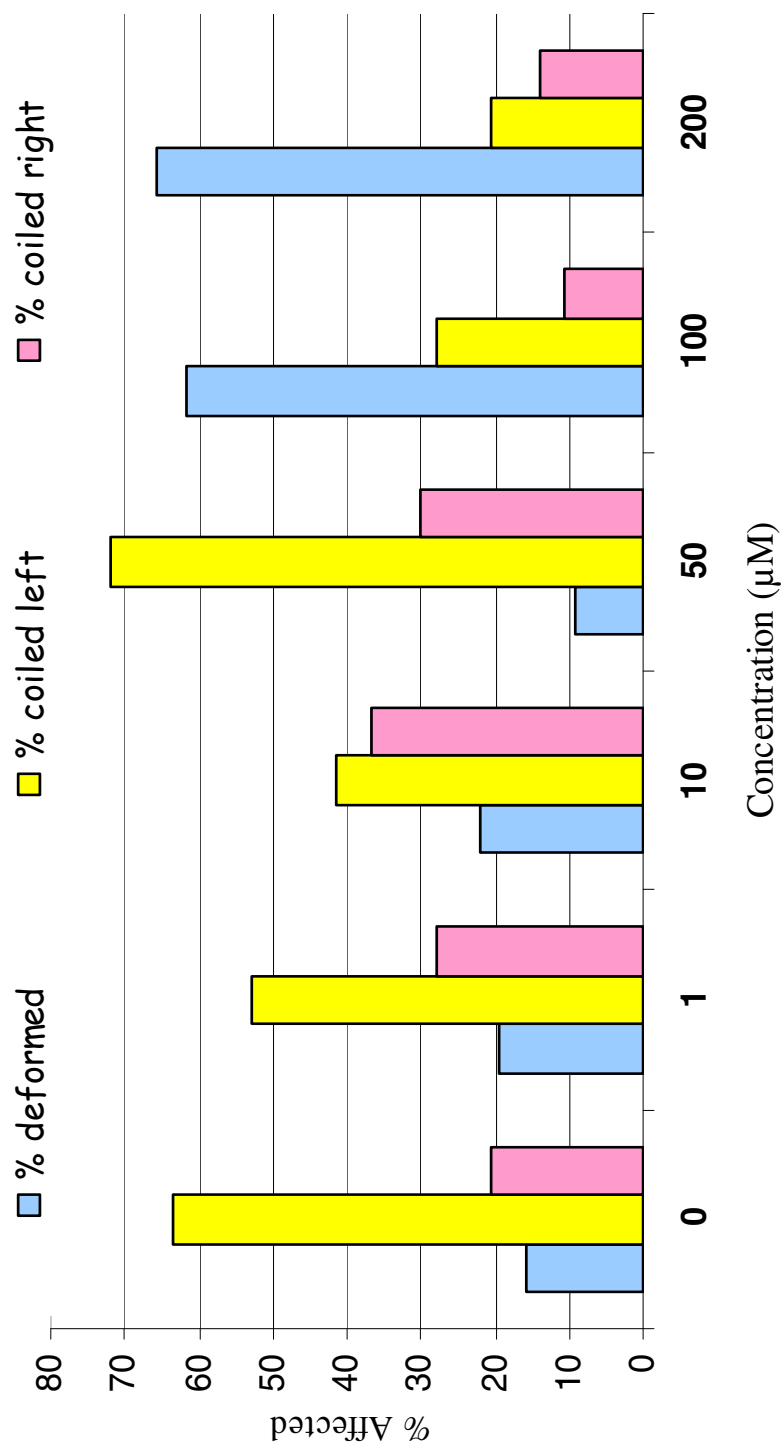


**Figure 6. Direction of Gut Coiling in Embryos Treated with Different Concentrations of Methotrexate.** The embryos treated with different concentrations of methotrexate were fixed at stage 45 (~98 hpf.) and categorized according to the direction or morphology of gut coiling. N = 83 - 88.



measurements of the neural tube were taken at the dorsal (A), ventral (D) and mediolateral (B and C) as shown in figure 7.

### *Homocysteine*

Figure 8 shows the average measurements of the thickness of the neural tube obtained at each of the above mentioned locations. Mediolateral sides were the thickest part of the neural tube while the dorsal side was the thinnest. At a homocysteine concentration of 25 mM, the dorsal side was considerably thinner (1.08 mm) compared to other concentrations and untreated embryos (4.13 mm). However, there does not seem to be any particular relationship between neural tube thickness and homocysteine concentration.

### *Methotrexate*

Neural tube thickness in relation to methotrexate concentrations is shown in figure 9. There is a substantial decrease in the thickness of the dorsal side as the concentration of methotrexate increases. The average thickness of the dorsal side in the untreated embryos was 5.88 mm, whereas in the embryos treated with 200  $\mu$ M methotrexate, this value was 2.71 mm. Also, there appears to be an increase in the thickness of the ventral side of the neural tube with increasing amounts of methotrexate (at 0  $\mu$ M – 4.2 mm and at 200  $\mu$ M – 5.5 mm). The thickness of the mediolateral sides

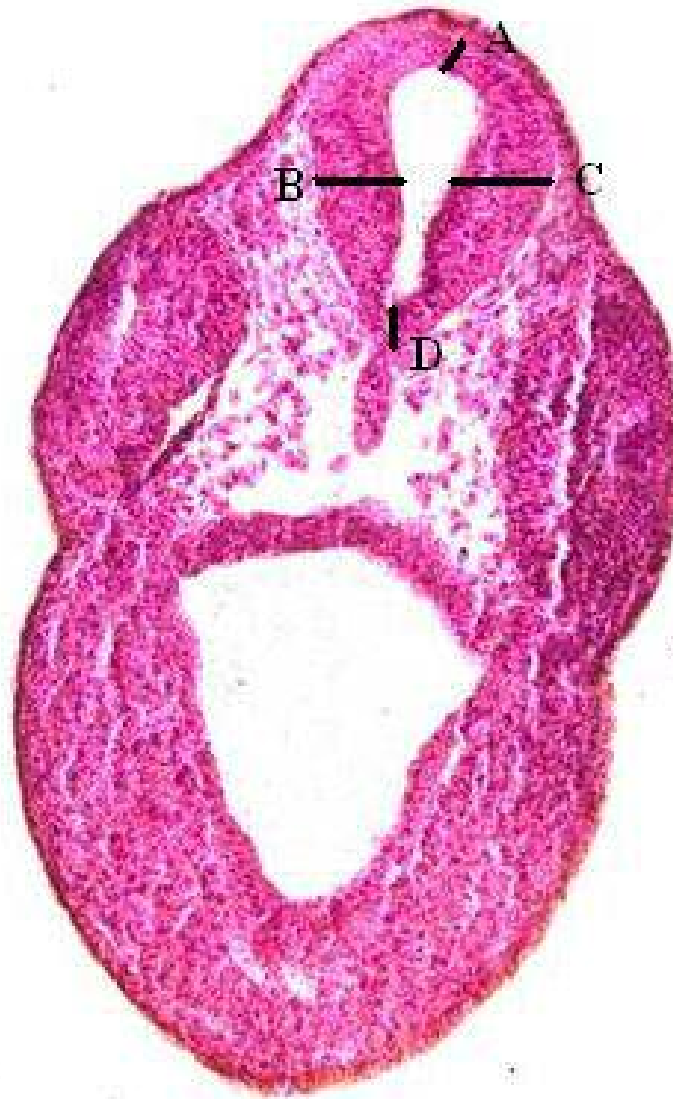


**Figure 7. Analysis of the Neural Tube.** Embryos treated with homocysteine and methotrexate were sectioned at stage 27 (~30 hpf.) and the neural tube was measured at dorsal (A), ventral (D) and mediolateral (B and C) widths.

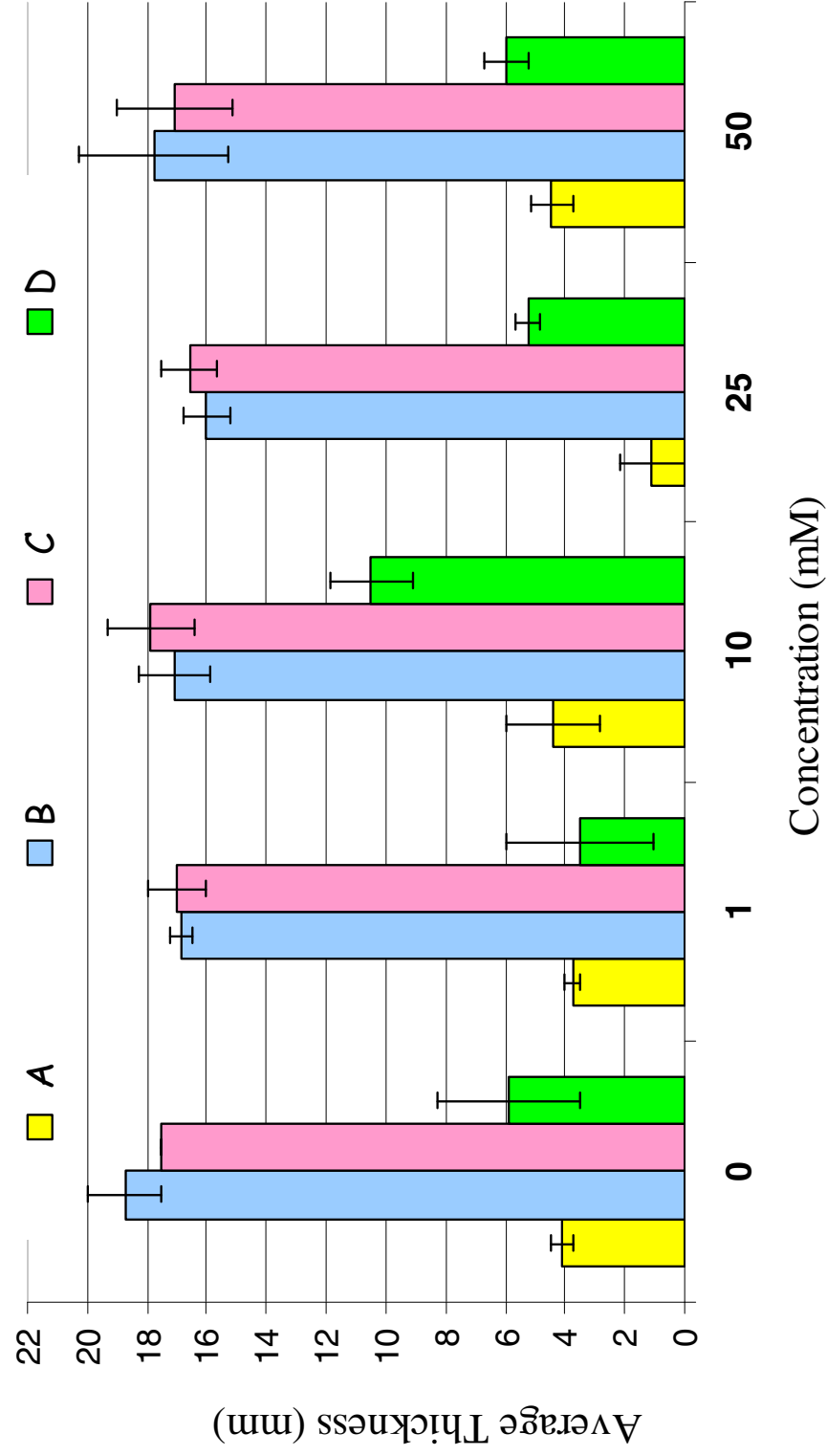


**Figure 8. Neural Tube Thickness at Different Homocysteine Concentrations.** The embryos treated with 0 mM, 1 mM, 10 mM, 25 mM and 50 mM homocysteine were fixed and sectioned at stage 27 (~30 hpf). The thickness of the neural tube neural tube was measured at dorsal (A), ventral (D) and mediolateral ends (B and C), as shown in figure #. The plotted values are the average  $\pm$  standard error. N= 2-5.

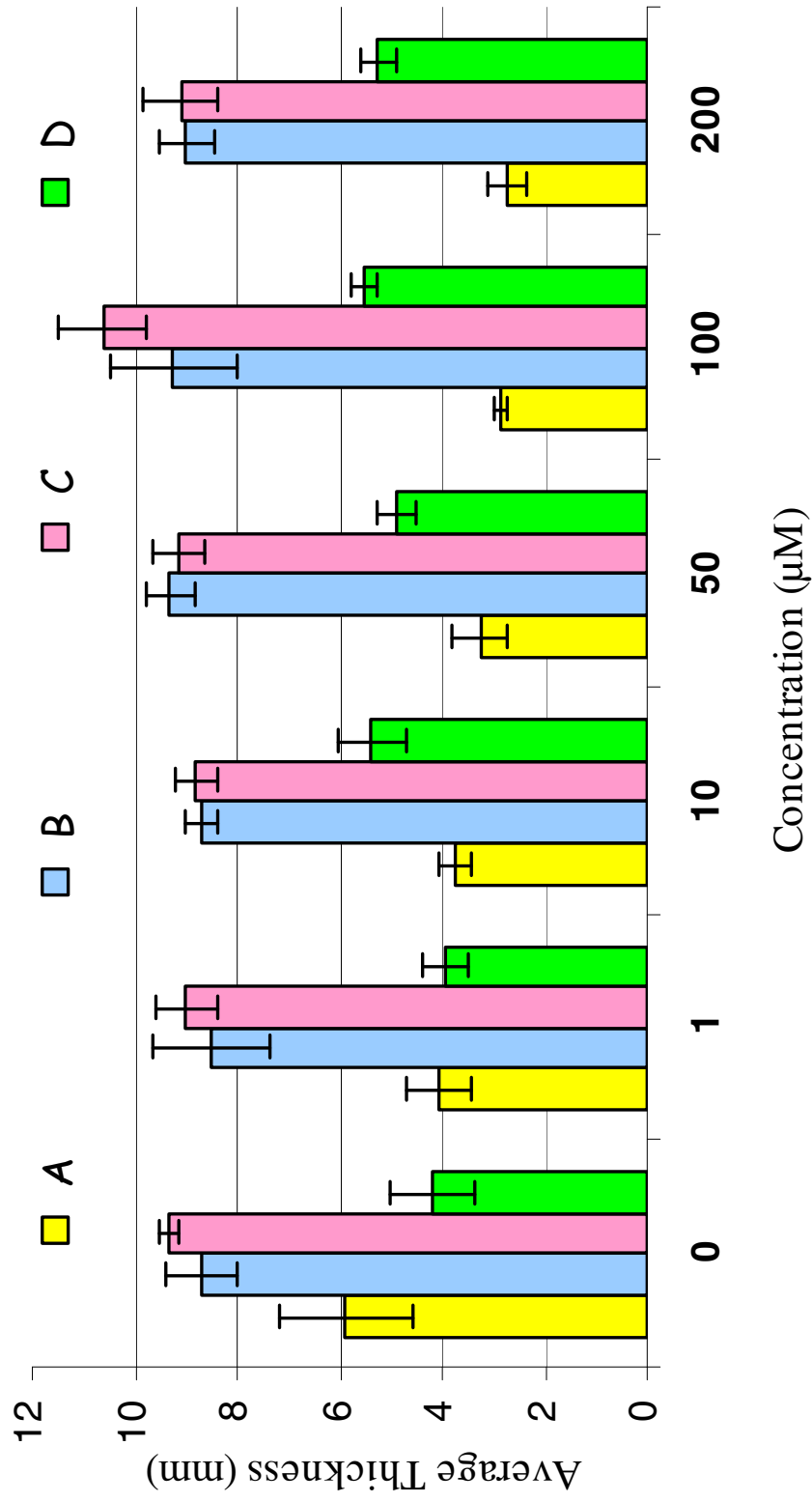


**Figure 9. Neural Tube Thickness at Different Methotrexate Concentrations.** The embryos treated with 0 μM, 1 μM, 10 μM, 50 μM, 100 μM and 200 μM concentrations of methotrexate were fixed and sectioned at stage 27 (~30 hpf). The thickness of the neural tube neural tube was measured at dorsal (A), ventral (D) and mediolateral ends (B and C), as shown in figure #. The plotted values are the average  $\pm$  standard error. N = 4 - 8.

remained about the same regardless of the methotrexate concentrations. In general, these embryo sections were of higher quality.

### ***Gene Expression Patterns in Xenopus Embryos with Altered Folate Metabolism***

Studies completed in this laboratory and at the National Institute of Environmental Health Sciences have shown that folate deficiency in cultured human fibroblast cells leads to alterations in the expression of genes, including those involved in the Wnt pathway. The Wnt signaling pathway controls patterning and cell fate determination during development (Wilt and Hake, 2004). It has been shown to be involved in the differentiation of the nervous system, skeletal muscles, cardiac cells, endoderm, cartilage and limbs (Gregory *et al.*, 2003). *Dkk-1* is an inhibitor of the canonical Wnt / beta-catenin signaling pathway and *Wnt-5A* is a positive activator of the pathway. Since both genes have been shown to be involved in *Xenopus* development it is possible that *Dkk-1* and *Wnt-5A* expression is altered in *Xenopus* embryos due to altered folate metabolism. In addition, we examined the expression of *Xtwist* and *Pax-3* genes. These genes are known to be involved in neural tube formation and there is evidence that *Pax-3* is linked in some way to the folate pathway (Tang *et al.*, 2003). The gene *Xbra* served as a negative control since it is a mesodermally expressed gene involved in gastrulation. The functions of all the genes used in this study and their embryonic patterns of expression are listed in Table 1.

Embryos were treated with 10 mM homocysteine and 100  $\mu$ M methotrexate and collected at stage 12 (gastrula), stage 20 (neurula) and stage 26 (tail bud). Whole-mount

*in situ* hybridization reactions were performed using different riboprobes according to table 1. Results for each gene were analyzed individually.

### *Pax 3*

*Pax-3* is a transcription factor which plays critical roles during neurogenesis (Takahashi *et al.*, 1992). Untreated and treated (10 mM homocysteine and 100  $\mu$ M methotrexate) embryos were grown to stage 12 (gastrula), a developmental stage where *Pax-3* expression pattern can be visualized as two patches situated at lateral ends of the embryo in the presumed site of the neural plate (Table 1). The level and pattern of staining in both untreated and homocysteine treated embryos were similar with two defined lateral patches at the dorsal side. The pattern of *Pax-3* expression in methotrexate treated embryos was similar in location to those of untreated embryos, but the staining was not restricted to a defined patch, rather spread from anterior to mid posterior (Figure 10). The expression pattern in cleared embryos did not seem any different from uncleared methotrexate embryos, but the level of *Pax-3* staining in homocysteine treated cleared embryos appeared diminished in comparison to untreated (figure 10). At higher magnification the above expression patterns were confirmed and the reduced level of hybridization in the homocysteine treated embryos is more apparent (Figure 11).

### *Dkk 1*

*Dkk-1* encodes a secreted protein which is required for head formation (Glinka *et al.*, 1998). Untreated and treated (10 mM homocysteine and 100  $\mu$ M methotrexate)

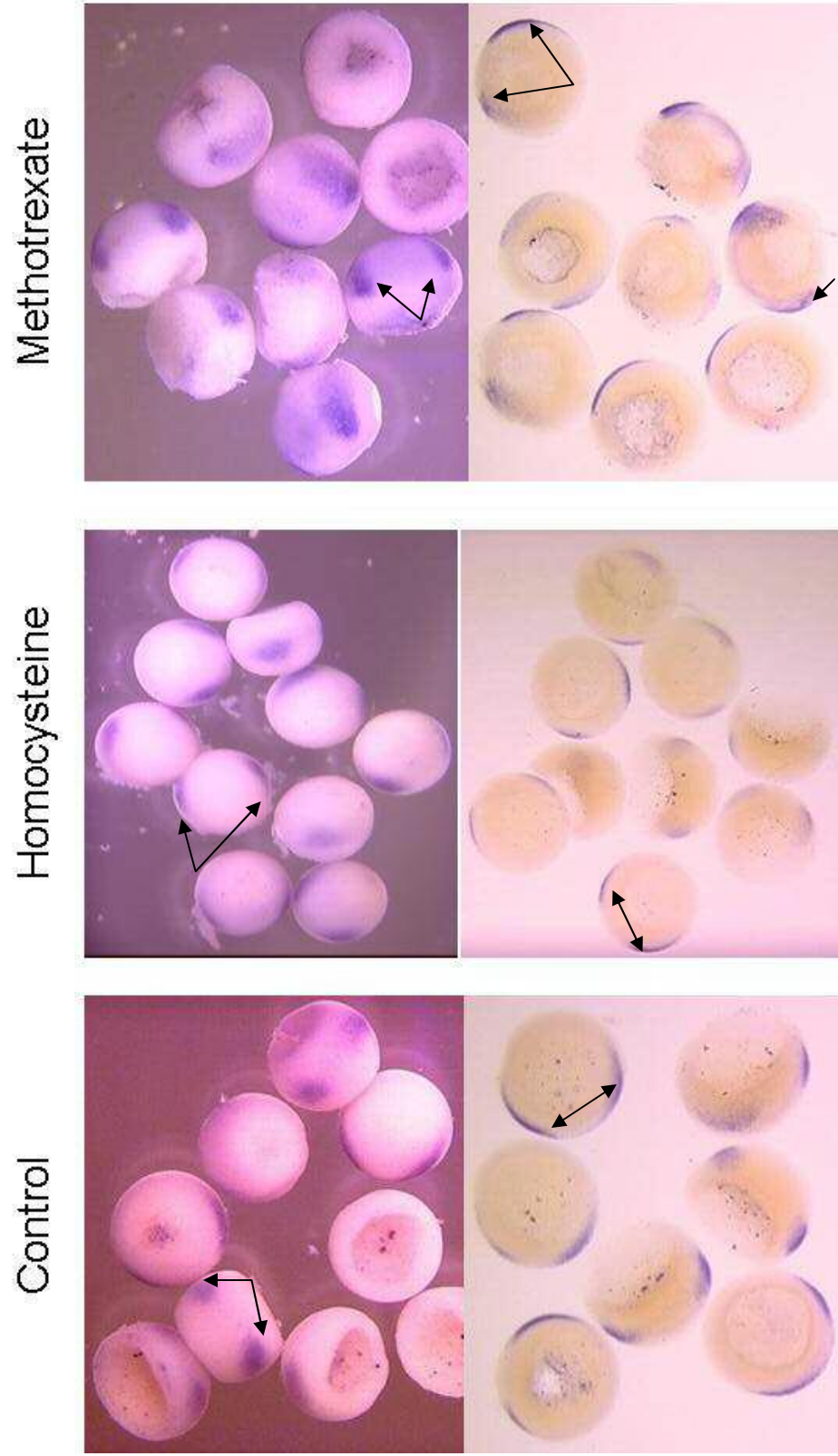


**Figure 10. Expression Pattern of Pax-3 in Treated and Untreated Embryos.** *In situ* hybridization was performed on treated (10 mM homocysteine and 100  $\mu$ M methotrexate) and untreated embryos at stage 12 (gastrula) using a Pax-3 riboprobe. Embryos were analyzed by light microscopy. The top panel shows embryos that are uncleared and bottom panel includes embryos cleared in BB/BA. Arrows indicate areas of specific staining.

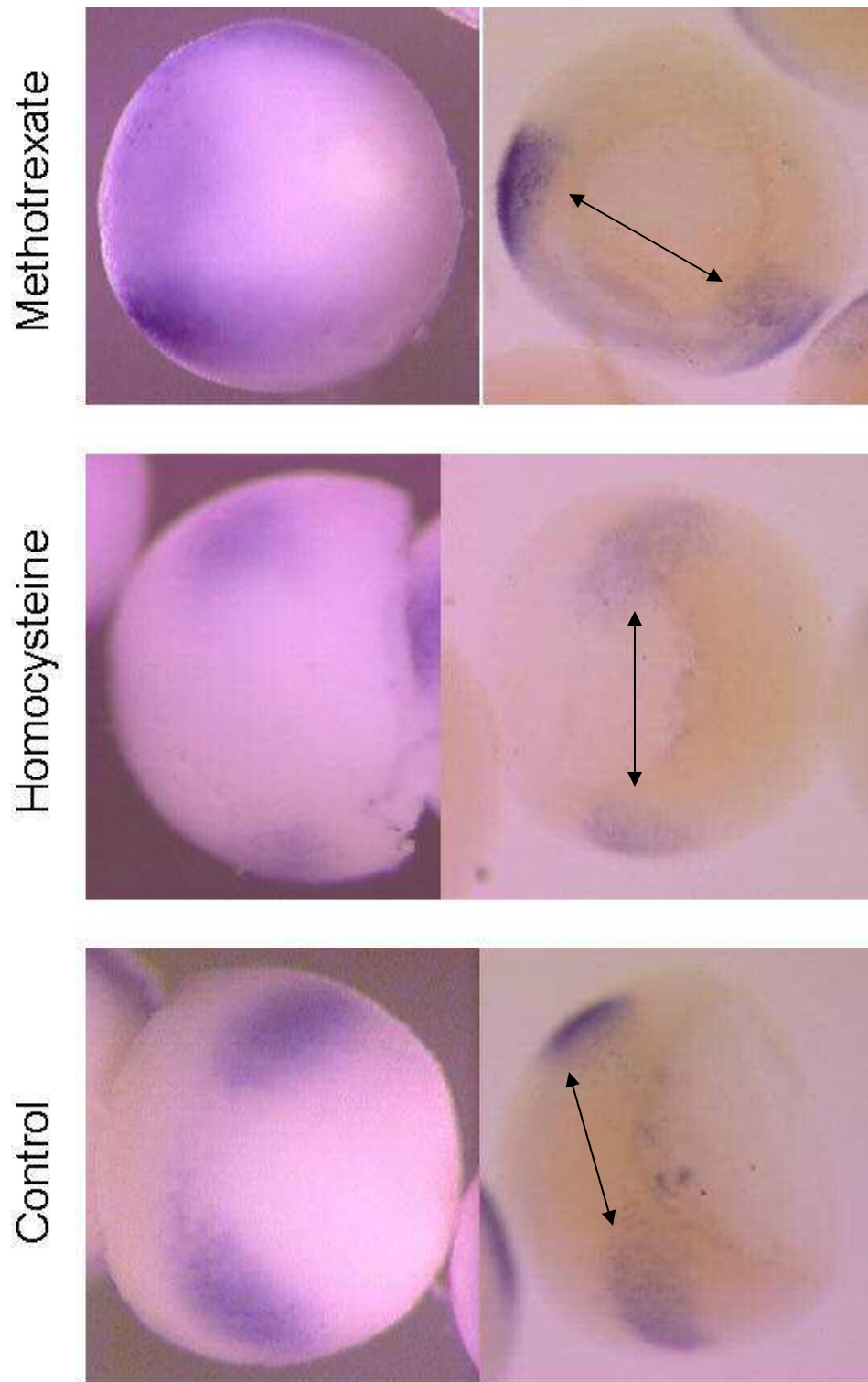


**Figure 11. Expression Pattern of *Pax-3* in Treated and Untreated Embryos Under High Magnification.** Same as in figure # but under higher magnification, 100x.



embryos grown to stage 12 were used to examine *Dkk-1* expression pattern. The pattern can be visualized at the anterior end with two streaks extending dorsally (Table 1). The treated and untreated embryos displayed a very weak staining pattern in the expected region (Figure 12) in comparison to the published data (Glinka *et al.*, 1998). It is likely that our embryos were at an earlier stage as evident by the large blastopore in comparison to that seen in *Dkk-1* stained embryos in table 1. However, it appeared that the staining was darker in untreated embryos compared to homocysteine and methotrexate treated embryos (Figure 12). Examining cleared embryos under higher magnification verified these findings (Figure 13). Moreover, it appeared that the level of expression in homocysteine was less than methotrexate. These results suggest that *Dkk-1* transcript levels are reduced in methotrexate and homocysteine treated embryos.

### *Xtwist*

*Xtwist* is a transcription factor expressed in the neural crest (Hopwood *et al.*, 1989). The treated (10 mM homocysteine and 100  $\mu$ M methotrexate) and untreated embryos were grown to stage 26 to examine *Xtwist* expression pattern. *Xtwist* is known to be expressed in neural tube, notochord, four cranial neural crests (mandibular, hyoid, anterior and posterior branchial crest), somites and neural crest cells, (Table 1). Comparing the treated (homocysteine and methotrexate) and untreated embryos, there appears to be no difference in the expression pattern. The pattern was prevalent in the neural tube, somites and head crests. But in some untreated embryos, the somites seem to be stained less than the treated embryos. It was difficult to compare these embryos as the

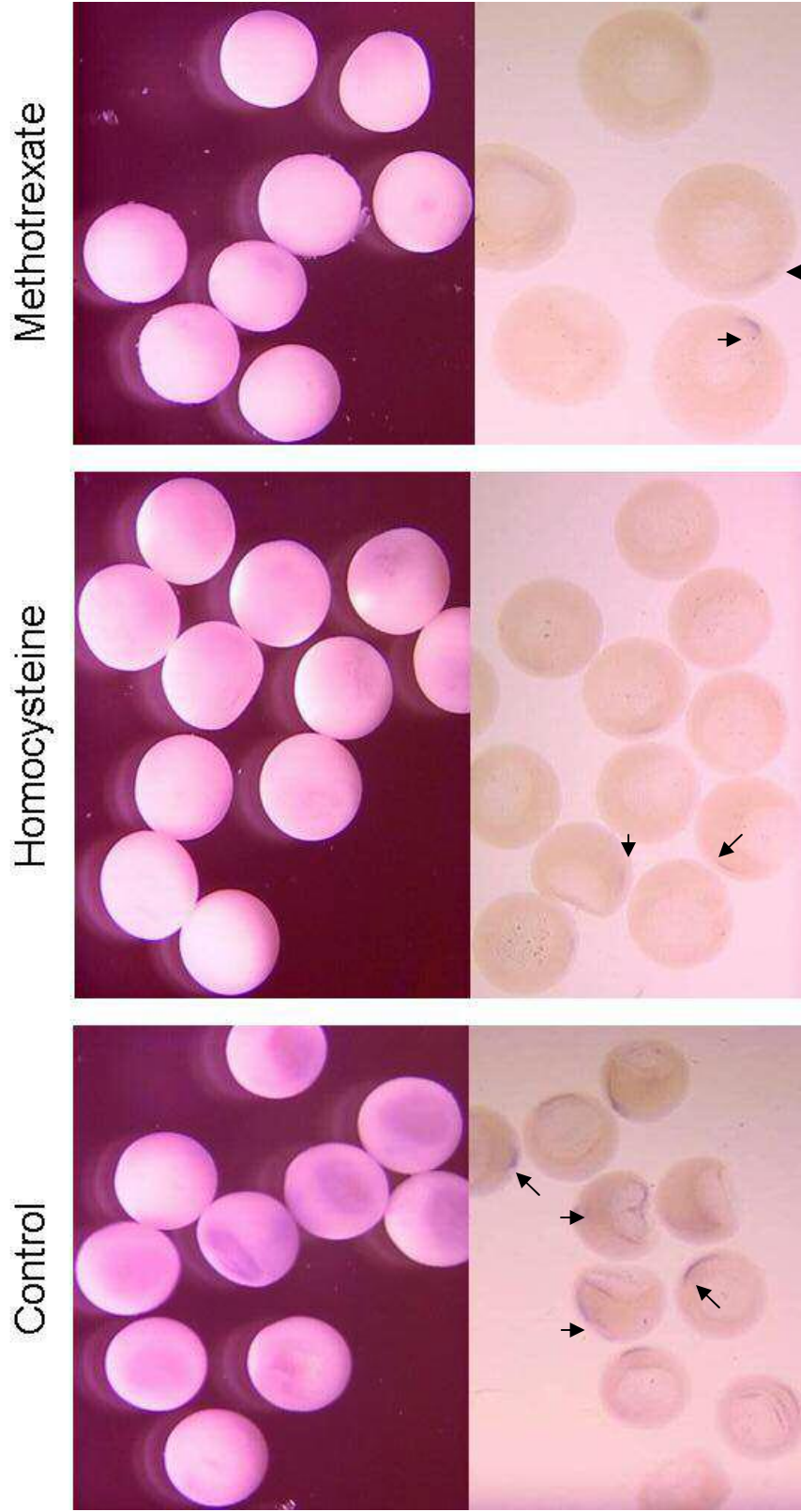


**Figure 12. Expression Pattern of *Dkk-1* in Treated and Untreated Embryos.** In situ hybridization was performed on treated (10 mM homocysteine and 100  $\mu$ M methotrexate) and untreated embryos at stage 12 (gastrula) using a *Dkk1* riboprobe. Embryos were analyzed by light microscopy. The top panel shows embryos that are uncleared and bottom panel includes embryos cleared in BB/BA. Arrows indicate areas of specific staining.

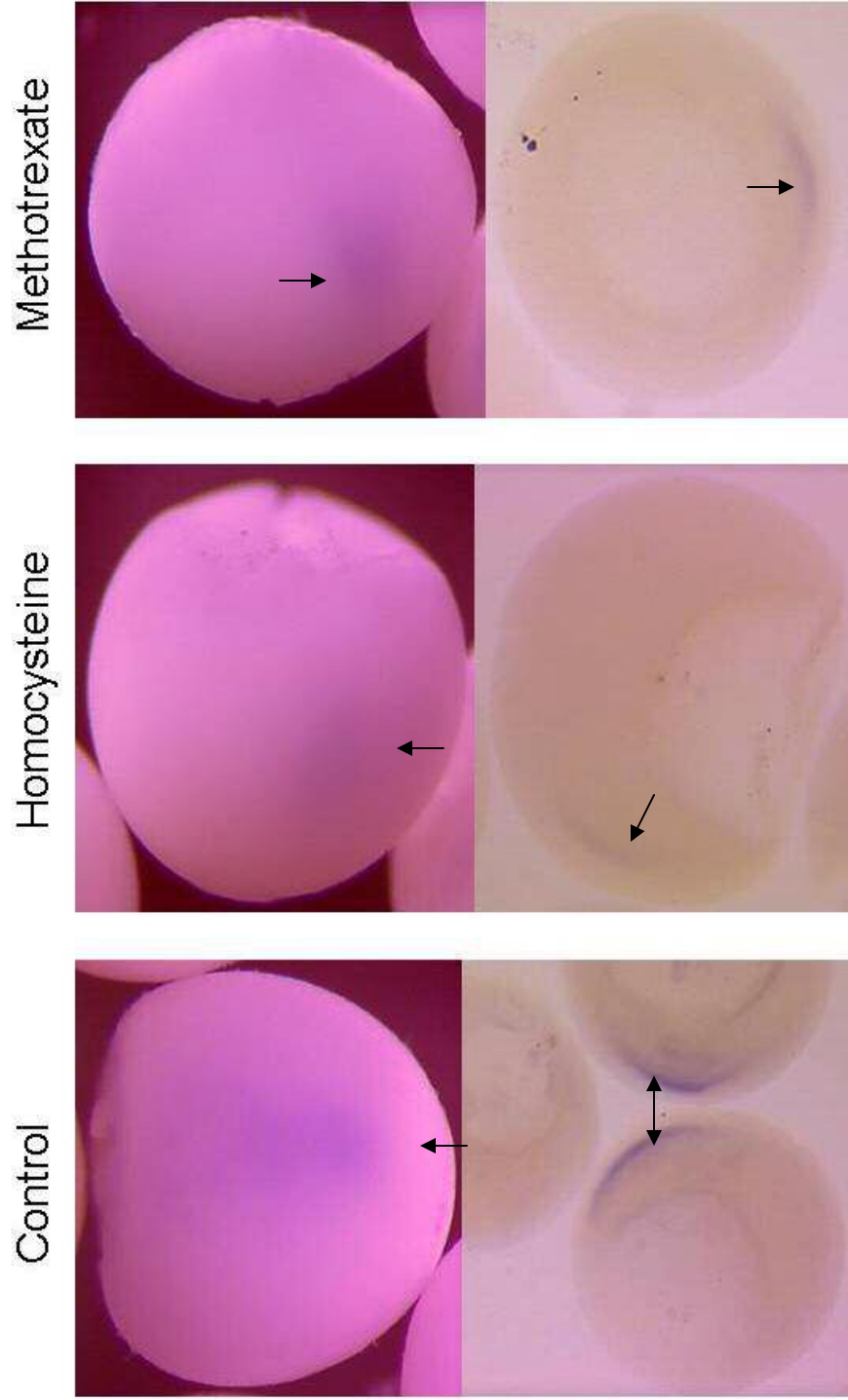


**Figure 13 Expression Pattern of *Dkk-1* in Treated and Untreated Embryos Under High Magnification.**  
Same as in figure # but under higher magnification, 100x.

expression pattern is quite complicated (Figure 14 and 15).

### *Xbra*

*Xbra* is a mesodermal transcription factor involved in regulating early Hox expression (Smith *et al.*, 1991). To examine the *Xbra* expression pattern 10 mM homocysteine and 100  $\mu$ M methotrexate treated and untreated embryos were grown to stage 12 (11 hpf). Since *XBra* is a mesodermal transcription factor, the normal pattern is displayed within the mesoderm cells surrounding the blastopore (Table 1). *XBra* expression level and pattern in the homocysteine treated embryos was uniform and similar to the untreated controls. Though the methotrexate treated embryos also stained around the yolk plug, the expression pattern included an extension , the notochord, (Figure 16 and 17 arrows ) and the staining level was less, which is more evident in the cleared embryos (Figure 16 and 17). However, the pattern was slightly different and the yolk plug was considerably smaller compared to the untreated and homocysteine treated embryos. These observations indicate that the methotrexate treated embryos were a later gastrula stage, compared to the untreated and homocysteine treated embryos.

### *Wnt-5A*

*Wnt-5A* encodes secreted signaling proteins involved in axis induction (Moon *et al.*, 1999). Homocysteine and methotrexate treated embryos were grown to stage 20 (neurula) to analyze *Wnt-5A* expression pattern. The treated (10 mM homocysteine and 100  $\mu$ M

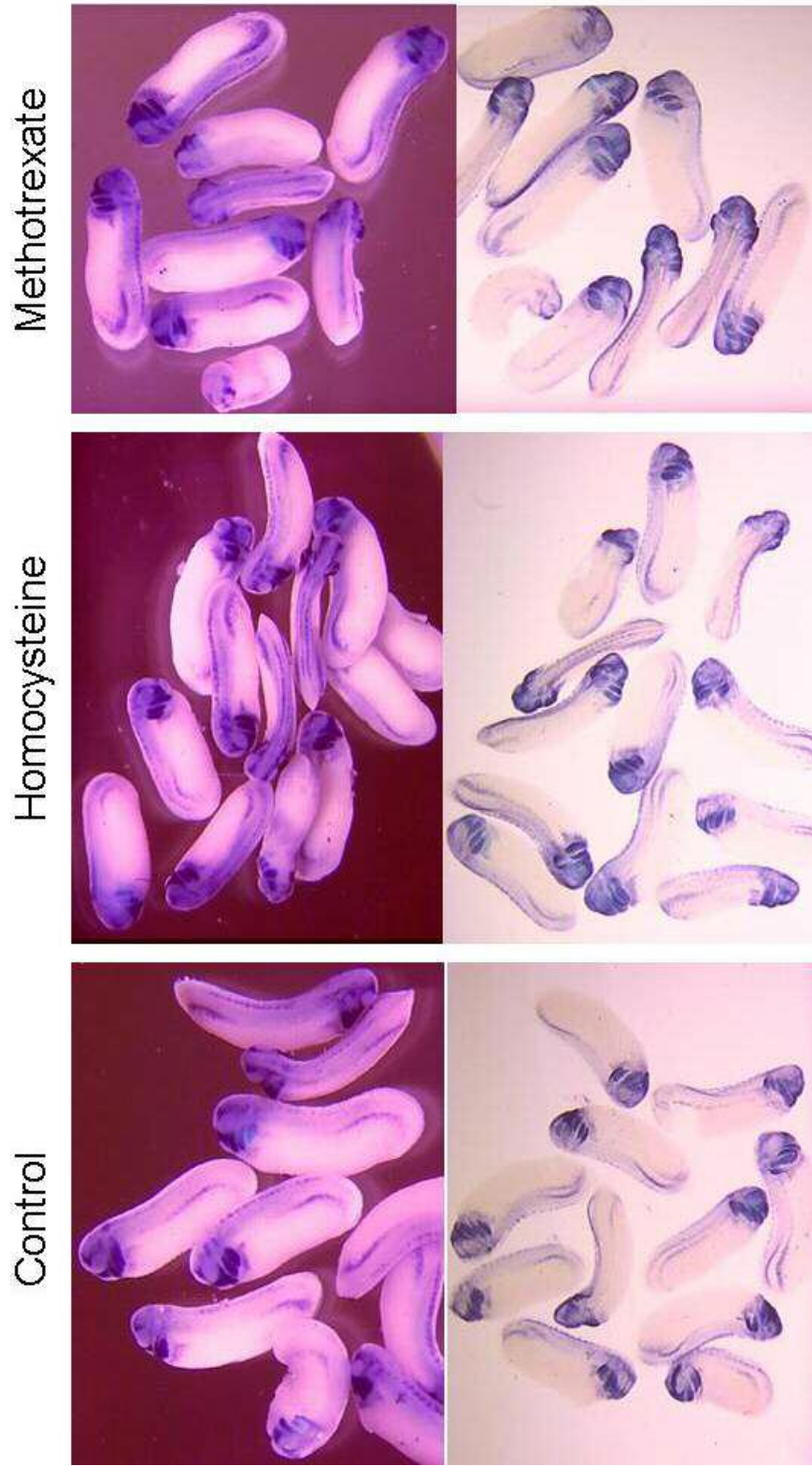


**Figure 14. Expression Pattern of *Xtwist* in Treated and Untreated Embryos.** In situ hybridization was performed on treated (10 mM homocysteine and 100  $\mu$ M methotrexate) and untreated embryos at stage 26 (tail bud) using a *Xtwist* riboprobe. Embryos were analyzed by light microscopy. The top panel shows embryos that are uncleared and bottom panel includes embryos cleared in BB/BA.



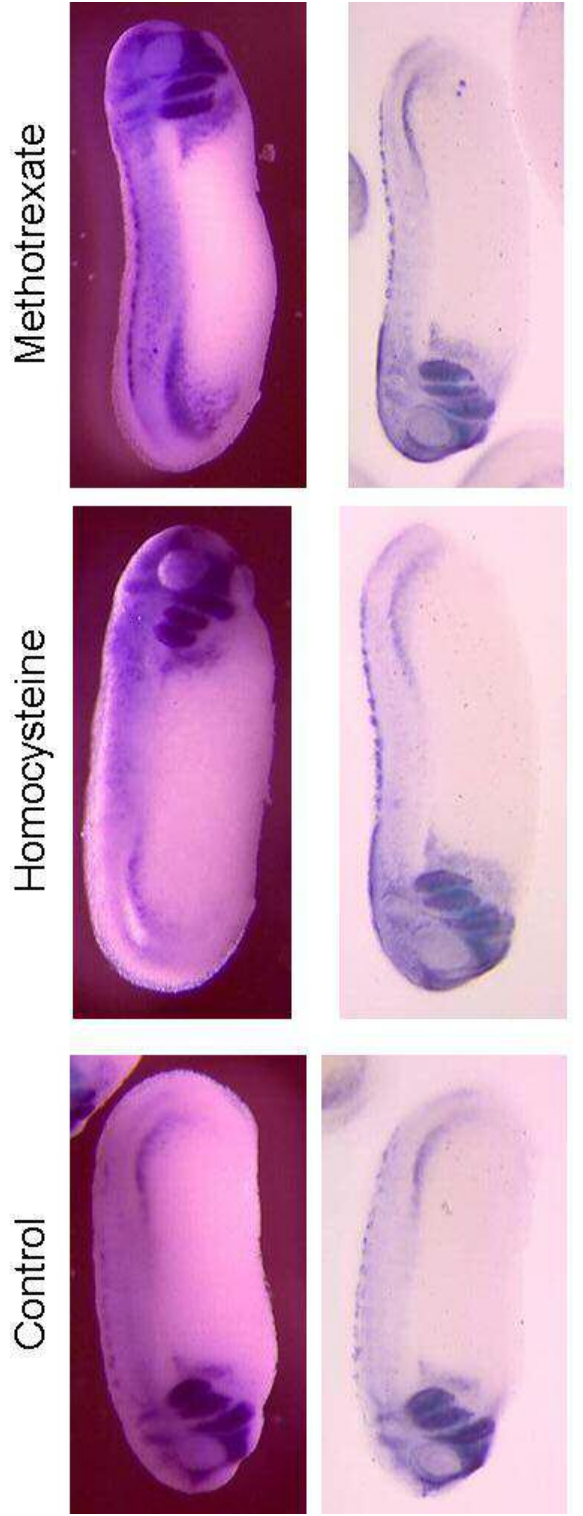


**Figure 15. Expression Pattern of *Xtwist* in Treated and Untreated Embryos Under High Magnification.** Same as in figure # but under higher magnification, 100x.

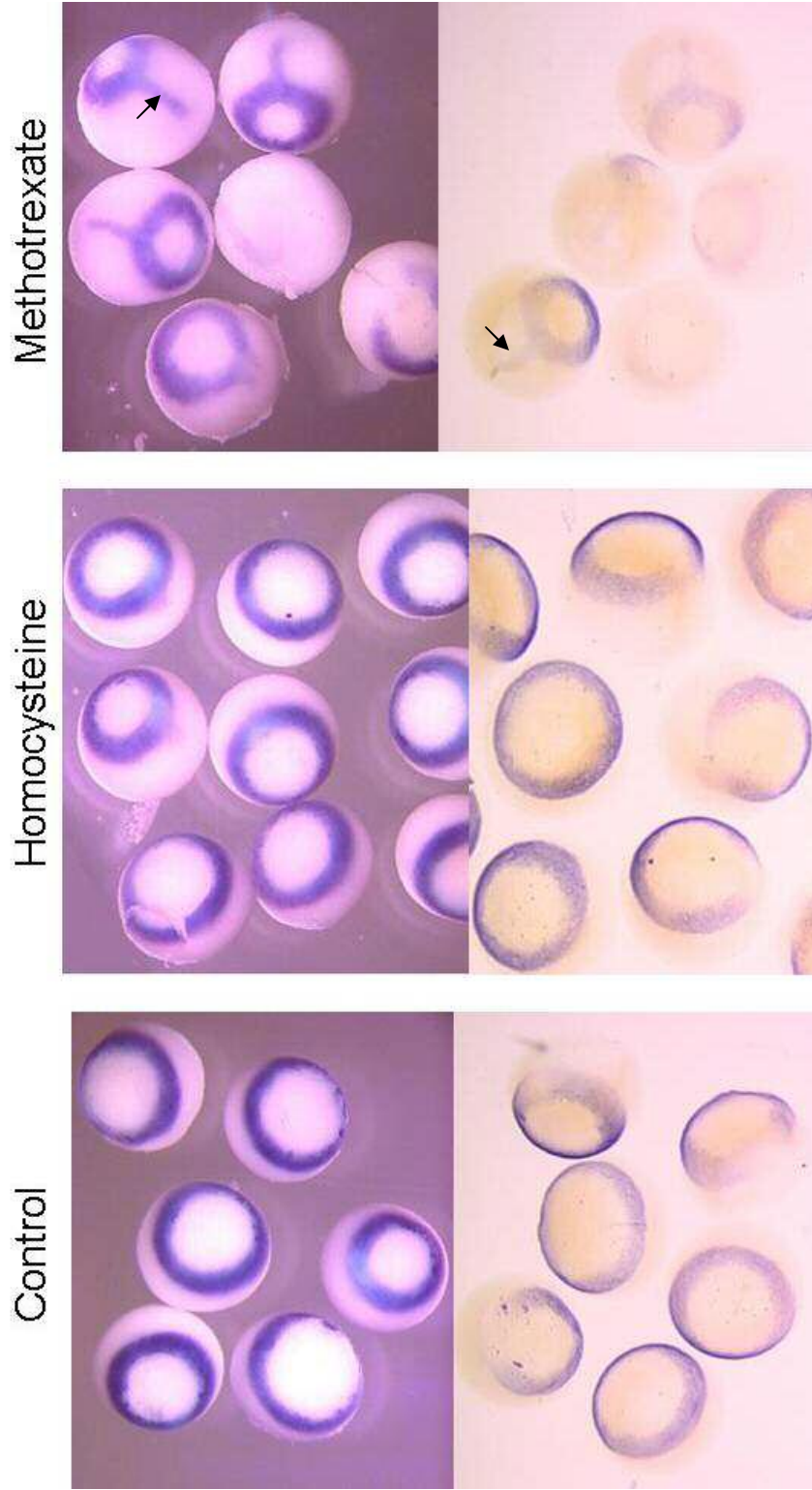


**Figure 16. Expression Pattern of *Xbra* in Treated and Untreated Embryos.** In situ hybridization was performed on treated (10 mM homocysteine and 100  $\mu$ M methotrexate) and untreated embryos at stage 12 (gastrula) using a *Xbra* riboprobe. Embryos were analyzed by light microscopy. The top panel shows embryos that are uncleared and bottom panel includes embryos cleared in BB/BA. Arrows indicate areas of extended expression of staining.

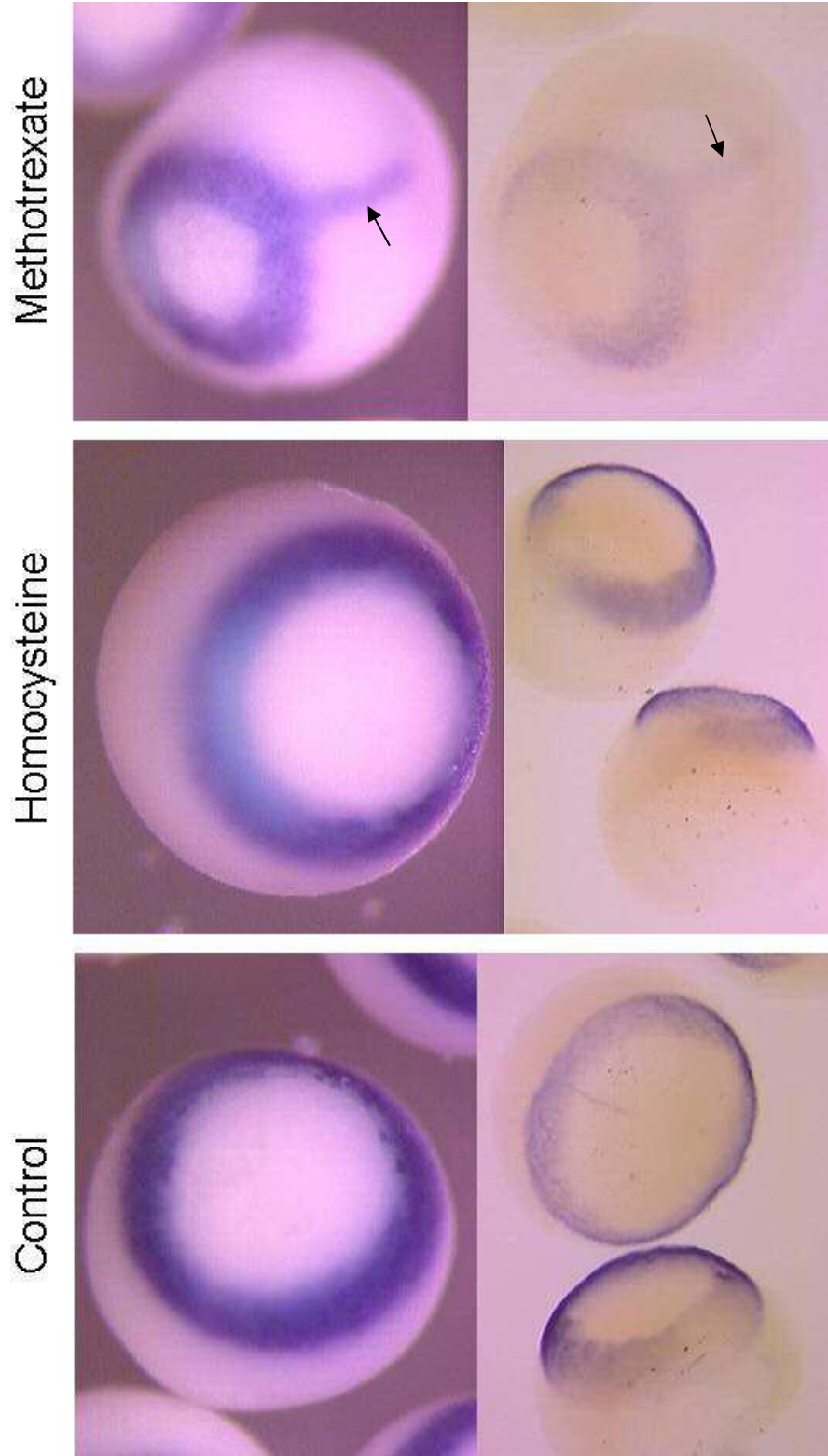


**Figure 17. Expression Pattern of *Xbra* in Treated and Untreated Embryos Under High Magnification. Same as in figure # but under higher magnification, 100x.**



methotrexate) and untreated embryos showed staining along the length of the neural tube (results not shown). Due to the inconsistent results achieved through the *in situ* hybridization protocol used at the time, these results were considered inconclusive and are not included.

## CHAPTER IV

### DISCUSSION

Approximately 1 out of every 2000 births are affected by neural tube defects in the United States. The most well-known environmental cause of neural tube malformation is folate deficiency in pregnant women (Northrup and Vocik, 2000). Although it has been established that administering folate to the pregnant mother reduces the prevalence of NTDs by as much as 48% (Daly *et al.*, 1995), the underlying mechanism is unclear. Therefore, a systematic approach based on expression patterns of genes is required to understand the mechanisms underlying folate-related birth defects. The goal of this study was to determine if altered folate metabolism during early development leads to changes in the expression of selected genes.

*Xenopus laevis* embryos were treated with different concentrations of homocysteine and methotrexate and their gross morphology including direction of gut coiling and neural tube thickness was analyzed. *In situ* hybridization was performed in treated and untreated embryos to analyze changes in expression patterns of the genes *Dkk-1*, *Pax-3*, *XBra*, *Xtwist* and *Wnt-5A*. It was evident that treatment with homocysteine and methotrexate lead to developmental defects consistent with folate deficiency. Gene expression patterns of *Xbra* and *Xtwist* was not affected by folate deficiency while *Dkk-1* and *Pax-3* expression appeared to be down regulated.

## ***Homocysteine and Methotrexate Cause Morphological Defects and Delayed Development***

It is not possible to deplete the folate naturally present in the egg, thus available to the growing embryo. In order to overcome this problem, we attempted to alter folate metabolism and mimic low levels of folate using the compounds methotrexate and homocysteine, respectively. Methotrexate inhibits the folate pathway enzyme, dihydrofolate reductase. As a consequence, there is a reduction in dTMP and methionine biosynthesis and an associated increase in homocysteine (Figure 1). The increased levels of homocysteine which are associated with NTDs, cancer, heart conditions and Alzheimer disease (Ernest *et al.*, 2002) mimic the conditions of blocking the folate pathway.

To assess the effects homocysteine and methotrexate have on *Xenopus* development, we examined gross morphology, gut coiling and neural tube thickness. In a previous study, methotrexate treatment of *Xenopus* embryos caused mis-coiling of the gut, microphthalmia, microencephaly and hydroencephaly (Bantle *et al.*, 1990). In chick embryos homocysteine treatment of chicken embryo lead to heart and neural tube defects (Afman *et al.*, 2003). And, mouse embryos lacking the *Folbp1* were found to have severe developmental defects including small embryos, a fewer number of somites, failure of the neural tube to fuse cranially and disruptions in palate formation (cleft palate) and upper lip (cleft lip). Also, *Folbp1* nullizygosity was found to be lethal as these embryos died in utero around gestational day 10 (Tang and Finnell, 2003; Piedrahita *et al.*, 1999). Based on these findings, we expected homocysteine and methotrexate treated *Xenopus* embryos

would exhibit similar morphological defects to that of folate deficient embryos as detected in these studies.

We found that homocysteine at higher concentrations was capable of arresting development at or around the time of gastrulation. When analyzing later stage embryos it was evident that homocysteine slowed the development of these embryos and caused numerous deformities such as small eyes, small bodies, kinked backs and gut deformities. Embryos treated with methotrexate exhibited similar morphological abnormalities. The percent mortality in homocysteine treated embryos ranged between 12 % - 15 %, whereas untreated remained at 7%. Methotrexate treated embryos had a percent mortality ranging from 3.9 % - 8.9%. The untreated embryos in the methotrexate had a percent mortality of 1.7%. It was evident homocysteine and methotrexate caused percent mortality to double in treated embryos compared to untreated. But, there did not appear to be a correlation between higher concentration and increased mortality. These results indicate both homocysteine and methotrexate effect development in a manner similar to that observed in development of other organisms subjected to compromised folate metabolism.

Guts in *Xenopus* start to coil at stage 41. By stage 45 the gut has acquired the proper coiling orientation. The gene *FoxF1* was found to be important in gut coiling and orientation. *FoxF1* is expressed in lateral plate mesoderm and later in visceral mesoderm. The absence of this gene has resulted in lack of proliferation and differentiation of the lateral plate and visceral mesoderm cells and impaired gut morphogenesis (Tseng *et al.*, 2004). Furthermore, *Xnr-1*, *XPitx2* and homeobox genes *Pdx1* and *Cdx2* are also found to be involved in gut morphogenesis (Beck, 2002). Methotrexate treatment has been shown

to result in randomization in the direction of gut coiling *Xenopus* embryos (Bantle *et al.*, 1990). One possibility is that methotrexate is affecting the expression of one or more of the genes listed above.

In our study of the effects of homocysteine on gut coiling most of the untreated embryos had a left coiled pattern and as the concentration of homocysteine increased the percent coiling to the left decreased. This was due both to an increase in the number of guts coiling to the right and the number of with deformed or mis-coiled guts. Methotrexate treated embryos showed similar effects with the increase of mis-coiled or deformed guts and decrease of guts coiling to the left as the concentration of methotrexate increased. The guts coiling to the right increased up to 10  $\mu$ M methotrexate and then at higher concentrations decreased. It is hard to explain why at 50  $\mu$ M methotrexate the number of guts coiling to the left increased dramatically while the number of deformed guts decreased. This very well could be due to an error in scoring such that right coiling guts were recorded as left.

Neurulation in chordates includes the formation of neural plate, neural folds and neural tube. The neural tube will develop into the future brain and spinal cord. The neural plate forms as a central strip of surface ectoderm cells, just above notochord. These cells gradually fold inward, forming neural folds and eventually breaks free of the surface ectoderm. The closing process of neural tube is very critical as defects in closure may results in spina bifida and other NTD (Colas and Schoenwolf, 2001). The most well known environmental cause of neural tube malformation is folate deficiency in pregnant women (Northrup and Volcik, 2000). Nullizygous *Folbp1* mice were found to have NTD

and craniofacial abnormalities such as cleft lip and cleft palate (Tang and Finnell, 2003). The defects in the neuroepithelium include lack of formation of the forebrain or optical vesicles, reduced thickness of neuroepithelium to only a couple of cells layers, altered migration of neural crest cells and lack of neural tube fusion (Piedrahita *et al.*, 1999). Analyzing the gross morphology of treated and untreated *Xenopus* embryos, we did not observe any embryos with defects in neural tube closure. This could be due to the fact we did not know how *Xenopus* embryos with neural tube closure defects might appear. With more consideration, it is very possible such embryos were present within the treatment groups as severely deformed embryos that did not continue to develop. In order to determine if homocysteine or methotrexate treatment affects *Xenopus* embryos in a similar manner to that of folate deficiency, the neural tube thickness at four regions was measured at a later developmental stage in surviving embryos.

Within the methotrexate treated embryos mediolateral sides were the widest. The increase in ventral measurements did not correspond to increased methotrexate levels. The width of the dorsal side decreased with increasing concentration of methotrexate, suggesting that blocking dihydrofolate reductase could lead to failure of neural tube closure. Similarly, mediolateral measurements were also the largest among homocysteine treated embryos. However all four measurements fluctuated and were not correlated with homocysteine concentration. The fact that methotrexate treated embryos had overall larger neural tube measurements suggests that the embryos used for homocysteine treatment groups might not have been at the same developmental stage. Also, the

variability of the homocysteine samples could be due to reduced quality of the embryo sections.

These results along with that of gross morphological affects and gut coiling suggest treatment of embryos with homocysteine and methotrexate affect embryos in a similar manner to that of embryos with folate deficiency. This conclusion is based on the finding that homocysteine and methotrexate treated embryos showed a delay in development, altered morphology and at least in methotrexate treated embryos there was a decrease in the thickness of the dorsal side of the neural tube. Additionally, the effect on gut coiling corresponds to published findings regarding the treatment of methotrexate.

### ***Altered Folate Metabolism Cause Changes in Specific Gene Expression***

#### ***Patterns***

Paired box gene 3 (*Pax-3*) is expressed in the dorsal aspect of the neural tube, from the midbrain level throughout the entire neural axis (Takahashi *et al.*, 1992). *Pax-3* expression occurs during neural plate formation and establishes, in part, the appropriate spatial information for later arising cells such as neural crest cells (Bang, 1999). In the absence of this gene, defective differentiation of neuroepithelial cells lead to the failure of neural tube closure in both midbrain and hindbrain regions (Tang and Finnell, 2003). Furthermore, *Pax-3* expression in nullizygous *Folbp1* embryos is decreased compared to the wild type (Tang and Finnell, 2003). In our studies the reduction in *Pax-3* expression in homocysteine and methotrexate treated embryos suggests that these compounds mimic folate deficiency and cause a change in *Pax-3* expression consistent with the results

observed in *Folbp1* <sup>-/-</sup> mice. Also, this allowed us to examine to what extent the known neural tube formation genes such as *Pax-3* were affected in *Xenopus* embryos with altered folate metabolism. We found that the level of *Pax-3* staining in homocysteine treated embryos was reduced. In a separate *in situ* hybridization experiment a decreased level of expression was detected in methotrexate treated embryos (results not shown). However, in the study shown (Figure 10 and Figure 11), methotrexate did not reduce *Pax-3* expression, and in fact there was a broader pattern of staining. This is likely due to these embryos being at a later developmental stage. The earliest expression of *Pax-3* is detected as two patches situated at lateral ends of the embryo in the site of neural plate at stage 11 (Bang *et al.*, 1999). For this reason, we chose to examine *Pax-3* expression at stage 12. Because of the difficulty of growing embryos at exactly the same rate, the methotrexate treated embryos were collected at a late gastrula stage. Unfortunately, there were no untreated embryos at this later stage to compare to the methotrexate treated embryos. It will be necessary to repeat the *in situ* hybridization studies for *Pax-3* and ensure that treated embryos are developmentally matched to the untreated embryos.

### *Dkk-1*

*Dkk-1* is expressed in the head organizer and encodes a family of secreted Wnt inhibitors that antagonize Wnt signaling (Moon *et al.*, 1993). *Dkk-1* antibody injection into *Xenopus* zygotes results in microcephaly. *Dkk-1* is speculated to be required for head formation (Glinka *et al.*, 1998). Additionally, studies completed in this laboratory and at the National Institute of Environmental Health Sciences have shown that *Dkk-1*



expression is down regulated in folate deficient cultured human fibroblast cells (Katula *et al.*, Submitted).

The earliest expression of *Dkk-1* is seen in the early gastrula when it is expressed in the Spemann organizer (Glinka *et al.*, 1998). At stage 10, *Dkk-1* expression is detected in the deep cells within the Spemann organizer. At a later gastrula stage, *Dkk-1* is expressed in three domains. The most anterior expression seen is in cells that give rise to the liver. The strongest expression is visualized in prospective prechordal plate in a wing shaped pattern in the middle of the endomesoderm. The third domain consists of two longitudinal strips. At a later neural stage, *Dkk-1* expression is seen in the prechordal plate adjacent to the prospective forebrain, eyes and somites (Glinka *et al.*, 1998).

Generally, the expression level of *Dkk-1* is quite low. In this study, *Dkk-1* expression was detected only in the longitudinal strips. This is likely due to the embryos being at an earlier stage than the published examples (Table 1). Methotrexate treated embryos showed a diminished level of expression compared to that of untreated embryos. Homocysteine treated embryos had the same expression pattern in comparison to methotrexate with lighter staining, corresponding to reduced expression levels. It is possible that the smaller eyes evident in some of the embryos treated with high concentrations of homocysteine and methotrexate could be due to reduced levels of *Dkk-1* expression in prechordal plate during late neural stage.

### *Xbra*

*Xbra* is an early mesodermal transcription factor that controls the early *Hox* gene expression in animal-vegetal direction (Smith *et al.*, 1991). We chose to include this gene in our expression studies as it can be a useful control for the *in situ* hybridization protocol. We did not expect the expression pattern to change in treated embryos as *Xbra* is not involved in neuroectoderm. However, there is no published data regarding modifications in *Xbra* expression due to folate deficiency. For this reason, *Xbra* served not only as a good control but also a gene of experimental interest.

During gastrulation, *Xbra* expression is observed in mesodermal cells around the blastopore as a ring (Table 1). In this study, untreated and homocysteine treated embryos showed the same expression level and pattern. When these embryos were compared to methotrexate treated embryos, *Xbra* expression was reduced in the methotrexate treated embryos, especially in the cleared embryos. Also, the expression pattern was altered. This observed pattern is more typical of a later gastrula stage (Smith *et al.*, 1991). The smaller blastopore and the staining of the notochord in methotrexate treated embryos supports this conclusion. Thus, it is likely that the decreased staining in methotrexate treated embryos is a consequence of being at a later developmental stage.

### *Xtwist*

*Xtwist* is a transcription factor expressed in the neural crest cells (Hopwood *et al.*, 1989). Staining was observed in the notochord, neural tube, cranial neural crest and somites. No obvious differences were observed between the untreated and homocysteine

treated embryos in this study. However, on close examination there appeared to be greater staining of the somites in the homocysteine treated embryos compared to the untreated. Again, this could be due to a slight change in the developmental stage. Methotrexate treated embryos showed a similar expression level and pattern to that of the homocysteine treated embryos. These results suggest not all transcription factors expressed in the neural crest cells are affected by folate deficiency.

#### *Wnt-5A*

*Wnt-5A* is a member of the Wnt gene family that encodes for secreted signaling proteins. *Wnt-5A* signaling is involved in axis induction through modification in the morphogenetic movement of tissues (Moon *et al.*, 1993). Also, it has been found that *Wnt-5A* expression is up regulated in folate deficient cultured human fibroblast cells (Katula, submitted). At stage 20 (neurula) normal *Wnt-5A* expression is prominent in the anterior and the posterior ectoderm of the embryo (Moon *et al.*, 1993). The *in situ* hybridization performed with riboprobe *Wnt-5A* using our initial protocol resulted in the neural tube being stained in all treated (homocysteine and methotrexate) and untreated embryos. These results were considered inconclusive as we were unable to determine if the staining patterns seen was specific or unspecific staining due to leaving embryo in alkaline phosphatase substrate, NBT/BCIP, for a long period of time.

During this study many difficulties arose. Having a sufficient number of healthy embryos was most critical to the success of these studies. Not only a large number of healthy embryos were required, but embryos derived from the same female were

necessary. On numerous occasions, *Xenopus* females produced only a few eggs.

Therefore, we had to collect eggs from more than one female and more than one batch of eggs from each female. Many of these batches of eggs were not as healthy and did not generate viable embryos. This could very well be one of the reasons that some treatments did not produce uniform effects. Incidentally, this is a better representation of the human population where severity of the effects of folate deficiency is different among babies.

We also had numerous problems performing the *in situ* hybridization reactions. One of which, embryos were not showing specific staining. This problem was solved after following Mr. Daniel D. Brown's (graduate student at UNC - Chapel Hill) protocol. In the process of following the initial protocol many of the collected embryos were used up. As a result we did not have enough treated embryos at the same developmental stage to perform *in situ* hybridization with the riboprobe *Wnt-5A*. Also, the expression level of *Dkk-1* was quite low compared to the expression of genes such as *Xbra*. To achieve the desired level of staining for *Dkk-1*, the embryos were left in staining compounds for long periods of time. This increased background staining, making it more difficult to analyze the pattern and level of staining.

We found that homocysteine and methotrexate caused a delay in development. Such a delay was also observed in *Folbp1* nullizygous embryos. It is known that gene expression levels and patterns change with the developmental stage. To be certain that these genes are, indeed being affected, it will be important to perform *in situ* hybridization reactions at different times around the developmental period when the gene is normally expressed. If the change in expression pattern and level seen was due to

homocysteine and methotrexate treatment, the observed difference (increased or decreased) would be consistent throughout the entire time period. This would enable us to rule out the possibility that the expression patterns that were observed were due to the developmental stages. Also, a time course should be done to see to what extent the rate of development is affected in treated embryos and if at all, how long it takes for the underdeveloped embryos to exhibit normal development. Moreover, the *in situ* hybridized embryos should be sectioned to examine the level of expression at the cellular level and the amount of specific RNA transcript present in the embryos evaluated by quantitative RT-PCR. Finally, head structures of the embryos should be analyzed more closely for the presence of orofacial deformities.

In summary, we attempted to mimic folate deficiency in *Xenopus laevis* embryos by treatment with homocysteine and methotrexate and to analyze changes in gene expression. We found that homocysteine and methotrexate affects *Xenopus* embryo development in a manner similar to folate deficiency. Furthermore, our data indicate that homocysteine and methotrexate alter the expression of specific genes. These results suggest that the *Xenopus laevis* model system could possibly be ideal for investigating the link between folate deficiency and the molecular basis of developmental defects. They also suggest that folate deficiency affects development through changes in expression patterns of specific genes, specifically genes involved in or regulated by Wnt signaling. These results must be validated with additional studies.

## REFERENCES

1. Afman LA, Blom HJ, Van der Put NMJ, Van Straaten V. Homocysteine interference in neurulation: A chick embryo model. *Birth Defects Research* **67**: 421-428, 2003.
2. Anderson DJ. Lineages and transcription factors in specification of vertebrate primary sensory neurons. *Curr Opin Neurobiol* **9**: 517-524, 1999.
3. Antony AC, Hansen DK. Hypothesis: Folate-responsive neural tube defects and neurocristopathies. *Teratology* **562**: 42-50, 2000.
4. Bang AG, Papalopulu N, Goulding MD, Kintner C. Expression of Pax-3 in the lateral neural plate is dependent on a Wnt-mediated signal from posterior nonaxial mesoderm. *Developmental Biology* **212**: 366-380, 1999.
5. Bantle JA, Fort DJ, Rayburn JR, Deyoung DJ, Bush SJ. Further validation of FETAX: evaluation of the developmental toxicity of five known mammalian teratogens and non-teratogens. *Drug Chem Toxicol* **13**: 267-82, 1990.
6. Barbera JPM, Rodriguez TA, Greene NDE, Weninger WJ, Simeone A, Copp AJ, Beddington RSP, Dunwoodie S. Folic acid prevents exencephaly in Cited2 deficient mice. *Human Molecular Genetics* **11**: 283-293, 2002.
7. Beck F. Homeobox genes in gut development. *Gut* **51**: 450-454, 2002. .
8. Bienengraber V, Malek FA, Moritz KU, Fanghanel J, Gundlach KK, Weingartner J. Is it possible to prevent cleft palate by prenatal administration of folic acid? An experimental study. *Cleft Palate Craniofac J* **38**: 393-398, 2001.
9. Birn H, Selhub J, Christensen EI. Internalisation and intracellular transport of folate-binding protein in rat kidney proximal tubule. *Am J Physiol* **264**: 302–310, 1993.
10. Blount BC, Mack MM, Wehr CM, MacGregor JT, Niatt RA, Wang G, Wickramasinghe SN, Everson RB, Ames BN. Folate deficiency causes uracil misincorporation into human DNA and chromosome breakage: Implications for cancer and neuronal damage. *Proc Natl Acad Sci USA* **94**: 3290-3295, 1997.

11. Boot MJ, Steegers-Theunissen RPM, Poelmann RE, Van Iperen L, Lindemans J, Gittenberger-de Groot AC. Folic acid and homocysteine affect neural crest and neuroepithelial cell growth and differentiation in vitro. *Developmental Dynamics* **227**: 301-308, 2003.
12. Botto LD, Moore CA, Khoury MJ, Erickson JD. Neural-tube defects. *N Engl J Med* **341**: 1509-1519, 1999.
13. Branford WW, Essner JJ, Yost HJ. Regulation of gut and heart left-right asymmetry by context-dependent interactions between *Xenopus* lefty and BMBP signaling. *Developmental Biology* **223**: 291-306, 2000.
14. Butterworth CE. Folate status, women's health, pregnancy outcome and cancer. *J Am Coll Nutr* **12**: 438-441, 1993.
15. Chalmers AD and Slack JMW. Development of Gut in *Xenopus laevis*. *Developmental Dynamics* **212**: 509-521, 1998.
16. Chalmers AD and Slack JMW. The *Xenopus* tadpole gut: fate maps and morphogenetic movements. *Development* **127**: 381-392, 2000.
17. Clarke R, Smith AD, Jobst KA, Refsum H, Sutton L, Ueland PM. Folate, vitamin B12 and serum total homocysteine levels in confirmed alzheimers disease. *Arch Neurol* **55**: 1449-1455, 1998.
18. Colas JF, Schoenwolf GC. Towards a cellular and molecular understanding of neurulation. *Dev Dyn* **221**: 117-45, 2001.
19. Copp AJ, Brook FA, Estibeiro JP, Shum AS, Cockroft DL. The embryonic development of mammalian neural tube defects. *Prog Neurobiol* **35**: 363-403, 1990.
20. Czeizel AE, Dudas I. Prevention of the first occurrence of neural-tube defects by periconceptional vitamin supplementation. *N Engl J Med* **327**: 1832-1835, 1992.
21. Daly LE, Kirke PN, Molloy A, Weir DG, Scott JM. Folate levels and neural tube defects. Implications for prevention. *The Journal of the American Medical Association* **274**: 1698-702, 1995.
22. Dekker GA, de Vries JJ, Doelitzsch PM, Huijgens PC, Blomberg BM, Jakobs C, van Geijn HP. Underlying disorders associated with severe early onset preeclampsia. *Am J Obstet Gynecol* **173**: 1042-1048, 1995.

23. DeSesso JM, Scialli AR, Holson JF. Apparent lability of neural tube closure in laboratory animals and humans. *Am J Med Genet* **87**: 143-162, 1999.
24. Duthie SJ, Narayanan S, Blum S, Pirie L, Brand GM. Folate deficiency in vitro induces uracil misincorporation and DNA hypomethylation and inhibits DNA excision repair in immortalized normal human colon epithelial cells. *Nutr Cancer* **37**: 245-51, 2000.
25. Duthie SJ. Folic acid deficiency and cancer: mechanisms of DNA instability. *Br Med Bull* **55**: 578-92, 1999.
26. Ernest S, Christensen B, Gilfix BM, Mamer OA, Hosack A, Rodier M, Colmenares C, McGrath J, Bale A, Balling R, Sankoff D, Rosenblatt Ds, Nadeau JH. Genetic and molecular control of folate-homocysteine metabolism in mutant mice. *Mammalian Genome* **13**: 259-267, 2002.
27. Fleming A. and Copp AJ. Embryonic folate metabolism and mouse neural tube defects. *Science* **280**: 2107-2109, 1998.
28. Gamse J, Sive H. Vertebrate anteroposterior patterning: the *Xenopus* neurectoderm as paradigm. *BioEssays* **22**: 976-986, 2000.
29. Glinka A, Wu W, Delius H, Monaghan AP, Blumenstock C, Niehrs C. Dickkopf-1 is a member of a new family of secreted proteins and functions in head induction. *Nature* **391**: 357-62, 1998.
30. Gregory CA, Singh H, Perry AS, Prockop DJ. The Wnt signaling inhibitor dickkopf-1 is required for reentry into the cell cycle of human adult stem cells from bone marrow. *J Biol Chem* **278**: 28067-78, 2003.
31. Groves AK, Bronner-Fraser M. Neural crest diversification. *Curr Top Dev Biol* **43**: 221-258, 1999.
32. Hall BK. The Neural Crest in Development and Evolution. New York: Springer-Verlang, Inc. 313, 1999.
33. Harris MJ, Juriloff DM. Mini-review: toward understanding mechanisms of genetic neural tube defects in mice. *Teratology* **60**: 292-305, 1999.
34. Herbert V, Larrabee AR, Buchanan JM. Studies on the identification of a folate compound of human serum. *J Clin Invest* **41**: 1134–1138, 1962.



35. Hopwood ND, Pluck A, Gurdon JB. A *Xenopus* mRNA related to *Drosophila* (elatic) twist is expressed in response to induction in the mesoderm and the neural crest. *Cell* **59**: 893-903, 1989.
36. James SJ, Pogribna M, Pogribny IP, Melnyk S, Hine RJ, Gibson JB, Yi P, Tafoya DL, Swenson DH, Wilson VL, Gaynor DW. Abnormal folate metabolism and mutation in the methylenetetrahydrofolate reductase gene may be maternal risk factors for Down's syndrome. *Am J Clin Nutri* **70**: 495-501, 1999.
37. Joosten PHJL, Toepoel M, Mariman ECM, Van Zoelen EJJ. Promoter haplotype combinations of the platelet-derived growth factor  $\alpha$ -receptor gene predispose to human neural tube defects. *Nature Genet* **27**: 215-217, 2001.
38. Kamei T, Kohono T, Ohwada H, Takeuchi Y, Hayashi Y, Fukuma S. Experimental study of the therapeutic effects of folate, vitamin A and vitamin B12 on squamous metaplasia of the bronchial epithelium. *Cancer* **71**: 2477-2483, 1993.
39. Kazanskaya O, Glinka A, Niehrs C. The role of *Xenopus* dickkopf 1 in prechordal plate specification and neural patterning. *Development* **127**: 4981-4992, 2000.
40. Kirby ML, Turnage KL, Hays BM. Characterization of conotruncal malformations following ablation of 'cardiac' neural crest. *Anat Rec* **213**: 87-93, 1985.
41. Lawson A, Anderson H, Schoenwolf GC. Cellular mechanisms of neural fold formation and morphogenesis in the chick embryos. *Ant Rec* **262**: 153-168, 2001.
42. Le Douarin N, Kalcheim C. The neural crest. Second edition. Cambridge: Cambridge University Press. 1999.
43. Li D, Pickell L, Liu Y, Wu Q, Cohn JS, Rozen R. Maternal methylenetetrahydrofolate reductase deficiency and low dietary folate lead to adverse reproductive outcomes and congenital heart defects in mice. *Am J Clin Nutri* **82**: 188-95, 2005.
44. Luccock M, Daskalakis I. New perspectives on folate status: a differential role for the vitamin in cardiovascular disease, birth defects and other conditions. *Br J Biomed Sci* **57**: 254-260, 2000.

45. Lucock M. Folic Acid: Nutritional biochemistry, molecular biology, and role in disease processes. *Mol Genet and Metabol* **71**: 121-138, 2000.
46. Lucock MD, Daskalakis I, Lumb CH, Schorah CJ, Levene MI. Impaired regeneration of monoglutamyl tetrahydrofolate leads to cellular folate depletion in mothers affected by a spina bifida pregnancy. *Mol Genet Metabol*. **65**: 18-30, 1998.
47. Lucock MD, Hartley R, Smithells RW. A rapid and specific HPLC-electrochemical method for the determination of endogenous 5-Methyltetrahydrofolic acid in plasma using solid phase sample preparation with internal standardization. *Biomed Chromatogr* **3**: 58-64, 1989.
48. Melvin EC, George TM, Worley g, Franklin A, Mackey J, Viles K, Shah N, Drake CR, Enterline DS, McLone D, Nye J, Oakes WJ, McLaughlin C, Walker ML, Peterson P, Brei T, Buran C, Aben J, Ohm B, Bermans I, Qumsiyeh M, Vance J, Pericak-Vance MA, Speer MC. Genetic studies in neural tube defects. NTD Collaborative Group. *Pediatr Neurosurg* **32**: 1-9, 2000.
49. Monaghan AP, Kioschis P, Wu W, Zuniga A, Bock D, Poustka A, Delius H, Niehrs C. Dickkopf genes are co-ordinately expressed in mesodermal lineages. *Mechanisms of Development* **87**: 45-56, 1999.
50. Monsoro-Burg A, Wang E, Harland R. Msx 1 and Pax 3 cooperate to mediate FGF8 and Wnt signals during *Xenopus* neural crest induction. *Developmental Cell* **8**: 167-178, 2005.
51. Moon RT, Campbell RM, Christian JL, McGrew LL, Shih J, Fraser S. Xwnt-5A: A maternal Wnt that affects morphogenetic movements after overexpression in embryos of *Xenopus laevis*. *Development* **119**: 97-111, 1993.
52. Moury JD, Schoenwolf GC. Cooperative model of epithelial shaping and bending during avian neurulation: autonomous movements of the neural plate, autonomous movements of the epidermis, and interactions in the neural plate/epidermis transition zone. *Dev Dyn* **204**: 323-337, 1995.
53. Newport J, Kirschner M. A major developmental transition in early *Xenopus* embryos: I. Characterization and timing of cellular changes at the midblastula stage. *Cell* **30**: 675-686, 1982.

54. Northrup H, Volcik KA. Spina bifida and other neural tube defects. *Curr Probl Pediatr* **30**: 313-32, 2000.
55. Olshan AF, Shaw GM, Millikan RC, Laurent C, Finnell RH. Polymorphisms in DNA repair genes as risk factors for spina bifida and orofacial clefts. *Am J Med Genet A* **135**: 268-73, 2005.
56. Petri M, Roubenhoff R, Dallal GE, Nadeau MR, Selhub J, Rosenberg IH. Plasma homocysteine as a risk factor for atherothrombotic events in systematic lupus erythematosus. *Lancet* **348**: 1120-1124, 1996.
57. Piedrahita JA, Oetama B, Bennett GD, van Waes J, Kamen BA, Richardson J, Lacey SW, Anderson RGW, Finnell RH. Mice lacking the folic acid-binding protein Folbp1 are defective in early embryonic development. *Nature Genetics* **23**: 228-232, 1999.
58. Poelmann RE, Mikawa T, Gittenberger-de Groot AC. Neural crest cells in outflow tract septation of the embryonic chicken heart: differentiation and apoptosis. *Dev Dyn* **212**: 373-384, 1998.
59. Pufulete M, Emery PW, Sanders TA. Folate, DNA methylation and colorectal cancer. *Proc Nutr Soc* **62**: 437-45, 2003.
60. Racek J, Rusnakova H, Trefil L, Siala KK. The influence of folate and antioxidants on homocysteine levels and oxidative stress in patients with hyperlipidemia and hyperhomocysteinemia. *Physiol Res* **54**: 87-95, 2005.
61. Refsum H, Guttormsen AB, Fiskerstrand T, Ueland PM. Hyperhomocysteinemia in terms of steady state kinetics. *Eur J Pediatr* **157**: 45-49, 1998.
62. Resenquist TH, Ratashak SA, Selhub J. Homocysteine induces congenital defects of the heart and neural tube: effect of folic acid. *Proc Natl Acad Sci USA* **93**: 15227-15232, 1996.
63. Romerio SC, Linder L, Nyfeler J, Wenk M, Litynsky P, Asmis R, Haefeli WE. Acute hyperhomocysteinemia decreases NO bioavailability in healthy adults. *Atherosclerosis* **179**: 419-20, 2005.
64. Rosenquist TH, Ratashak SA, Selhub J. Homocysteine induces congenital defects of the heart and neural tube: effect of folic acid. *Proc Natl Acad Sci USA* **93**: 15227-15232, 1996.

65. Sausedo RA, Smith JL, Schoenwolf GC. Role of nonrandomly oriented cell division in shaping and bending of the neural plate. *J Comp Neurol* **381**: 473-488, 1997.
66. Schoenwolf GC, Alvarez IS. Roles of neuroepithelial cell rearrangement and division in shaping of the avian neural plate. *Development* **106**: 427-439, 1989.
67. Schoenwolf GC, Franks MV. Quantitative analyses of changes in cell shapes during bending of the avian neural plate. *Dev Biol* **105**: 257-272, 1984.
68. Schoenwolf GC, Smith JL. Epithelial cell wedging: A fundamental cell behavior contributing to hinge point formation during epithelial morphogenesis. In: Keller RE, Fristrom D, editors. Control of morphogenesis by specific cell behaviors. Seminars in developmental biology, Vol 1, pp. 325-334. London: W.B. Saunders Co. 1990.
69. Schoenwolf GC. Microsurgical analyses of avian neurulation: separation of medial and lateral tissues. *J Comp Neurol* **276**: 498-507, 1988.
70. Slattery ML, Potter JD, Samowitz W, Schaffer D, Leppert M. Methylene-tetrahydrofolate reductase, diet and risk of colon cancer. *Cancer Epidemiol Biomarkers Prevention* **8**: 513-518, 1999.
71. Smith JC, Price BM, Green J, Weigel D, Herrmann BG. Expression of a *Xenopus* homolog of Brachyury (T) is an immediate-early response to mesoderm induction. *Cell* **67**: 79-87, 1991.
72. Smith JL, Schoenwolf GC. Cell cycle and neuroepithelial cell shape during bending of the chick neural plate. *Anat Rec* **218**: 196-206, 1987.
73. Smith JL, Schoenwolf GC. Further evidence of extrinsic forces in bending of the neural plate. *J Comp Neurol* **307**: 225-236, 1991.
74. Smith JL, Schoenwolf GC. Notochordal induction of cell wedging in the chick neural plate and its role in neural tube formation. *J Exp Zool* **250**: 49-62, 1989.
75. Smith JL, Schoenwolf GC. Role of cell-cycle in regulating neuroepithelial cell shape during bending of the chick neural plate. *Cell Tissue Res* **252**: 491-500, 1988.

76. Smithells RW, Sheppard S, Schorah CJ. Vitamin deficiencies and neural tube defects. *Arch Dis Child* **51**: 944-950, 1976.
77. Steegers-Theunissen RP, Boers GH, Trijbels FJ, Finkelstein JD, Blom HJ, Thomas CM, Borm GF, Wouters MG, Eskes TK. Maternal hyperhomocysteinemia: a risk factor for neural-tube defects. *Metabolism* **43**: 1475-1480, 1994.
78. Stumpo DJ, Eddy RL, Jr., Haley LL, Sait S, Shows TB, Lai WS, Young WS, 3<sup>rd</sup>, Speer MC, Dehejia A, Polymeropoulos M, Blackshear PJ. Promoter sequence, expression, and fine chromosomal mapping of the human gene (MLP) encoding the MARCKS-like protein: identification of neighboring and linked polymorphic loci for MLP and MACS and use in the evaluation of human neural tube defects. *Genomics* **49**: 253-264.
79. Takahashi Y, Monsoro-Burq A, Bontoux M, Le Douarin NM. A role for Quox-8 in the establishment of the dorsoventral pattern during vertebrate development. *Proc Natl Acad Sci USA* **89**: 10237-10241, 1992.
80. Tang LS, Finnell RH. Neural and orofacial defects in Folbp 1 knockout mice. *Birth Defects Research* **67**: 209-218, 2003.
81. Tang LS, Wlodarczyk BJ, Santillano DR, Miranda RC, Finnell RH. Developmental consequences of abnormal folate transport during murine heart morphogenesis. *Birth Defects Res Part A Clin Mol Teratol* **70**: 449-58, 2004.
82. Tseng HT, Shah R, Jamrich M. Function and regulation of FoxF1 during *Xenopus* gut development. *Development* **131**: 3637-3647, 2004.
83. Van Aerts LA, Bloom HJ, Deabreu RA. Prevention of neural tube defects by and toxicity of L-homocysteine in cultured postimplantation rat embryo. *Teratology* **50**: 348-360, 1994.
84. Van der Put NM, Thomas CM, Eskes TK. Altered folate and vitamin B12 metabolism in families with spina bifida offspring. *QJM* **90**: 505-510, 1997.
85. Vismara C, Bacchetta R, Cacaotore B, Vailah G, Fascio U. Paraquat embryotoxicity in the *Xenopus laevis* cleavage phase. *Aquatic Toxicology* **55**: 85-93, 2000.
86. Wilt FH, Hake SC. *Principles Developmental Biology*. 60, 67-70, 2004.